Projection of future river runoffs in Eastern Atlantic Canada from Global and Regional climate models

Nicolas Lambert, Joël Chassé, Will Perrie, Zhenxia Long, Lanli Guo and John Morrison

Aquatic Resources Division
Fisheries and Oceans Canada
Gulf Fisheries Centre
343 Université Avenue, PO Box 5030
Moncton, New Brunswick, E1C 9B6

2013

Canadian Technical Report of Hydrography and Ocean Sciences 288

Fisheries and Oceans Canada | Pêches et Océans Canada

Canada

Canadian Technical Report of Hydrography and Ocean Sciences

Technical reports contain scientific and technical information of a type that represents a contribution to existing knowledge but which is not normally found in the primary literature. The subject matter is generally related to programs and interests of the Oceans and Science sectors of Fisheries and Oceans Canada.

Technical reports may be cited as full publications. The correct citation appears above the abstract of each report. Each report is abstracted in the data base *Aquatic Sciences and Fisheries Abstracts.*

Technical reports are produced regionally but are numbered nationally. Requests for individual reports will be filled by the issuing establishment listed on the front cover and title page.

Regional and headquarters establishments of Ocean Science and Surveys ceased publication of their various report series as of December 1981. A complete listing of these publications and the last number issued under each title are published in the *Canadian Journal of Fisheries and Aquatic Sciences*, Volume 38: Index to Publications 1981. The current series began with Report Number 1 in January 1982.

Rapport technique canadien sur l'hydrographie et les sciences océaniques

Les rapports techniques contiennent des renseignements scientifiques et techniques qui constituent une contribution aux connaissances actuelles mais que l'on ne trouve pas normalement dans les revues scientifiques. Le sujet est généralement rattaché aux programmes et intérêts des secteurs des Océans et des Sciences de Pêches et Océans Canada.

Les rapports techniques peuvent être cités comme des publications à part entière. Le titre exact figure au-essus du résumé de chaque rapport. Les rapports techniques sont résumés dans la base de données *Résumés des sciences aquatiques et halieutiques*.

Les rapports techniques sont produits à l'échelon régional, mais numérotés à l'échelon national. Les demandes de rapports seront satisfaites par l'établissement auteur dont le nom figure sur la couverture et la page de titre.

Les établissements de l’ancien secteur des Sciences et Levés océaniques dans les régions et à l'ad-ministration centrale ont cessé de publier leurs diverses séries de rapports en décembre 1981. Vous trouverez dans l'index des publications du volume 38 du *Journal canadien des sciences halieutiques et aquatiques*, la liste de ces publications ainsi que le dernier numéro paru dans chaque catégorie. La nouvelle série a commencé avec la publication du rapport numéro 1 en janvier 1982.

Canadian Technical Report of Hydrography and Ocean Sciences
No. 288

2013

Projection of future river runoffs in Eastern Atlantic Canada from Global and Regional climate models

by

Nicolas Lambert[1], Joël Chassé[2], Will Perrie[3], Zhenxia Long[3], Lanli Guo[3] and John Morrison[4]

[1]Direction des sciences océaniques et de l'environnement
Pêches et Océans Canada
Institut Maurice-Lamontagne
850, Route de la Mer, C.P. 1000
Mont-Joli, Québec, G5H 3Z4

[2]Aquatic Resources Division
Fisheries and Oceans Canada
Gulf Fisheries Centre
343 Université Avenue, PO Box 5030
Moncton, New Brunswick, E1C 9B6

[3]Fisheries and Oceans Canada
Bedford Institute of Oceanography,
Dartmouth, NS
B2Y 4A2, Canada

[4]Vynx Design Inc.
10559 McDonald Park Rd.
Sidney, British Columbia
Canada, V8L 3J2

Cat. No. Fs 97-18/288E 0711-6764 (Printed version)
Cat. No. Fs 97-18/288E-PDF 1488-5417 (on-line version)

Correct citation for this publication:

Lambert, N., Chassé, J., Perrie, W., Long, Z., Guo, L. and Morrison, J. 2013. Projection of future river runoffs in Eastern Atlantic Canada from Global and Regional climate models. Can. Tech. Rep. Hydrogr. and Ocean. Sci. 288: viii + 34 p.

Table of contents

List of Figures

List of Tables

Abstract

Lambert, N., Chassé, J., Perrie, W., Long, Z., Guo, L. and Morrison, J. 2013. Projection of future river runoffs in Eastern Atlantic Canada from Global and Regional climate models. Can. Tech. Rep. Hydrogr. and Ocean. Sci. 288: viii + 34 p.

Runoff from three Global Climate Models (GCMs) was used to determine the discharge of major rivers leading to the North-West Atlantic. The GCMs (CanESM2, GFDL-ESM2M and MPI-ESM-LR) simulated the future climate under the green gas emission scenarios from the IPCC AR5 (RCP 4.5 and RCP 8.5). Land surface models of the GCMs provided the information about the runoff over the ground and thus, were able to feed the calculations of river discharges over the study area. Data from two Regional Climate Models (RCMs) were also used for the same purpose but under the AR4 SRES A1B and A2 emissions scenarios. In the latter case, evaporation, precipitation and temperature allowed for the calculation of river runoffs. We used a simple hydrologic model based on the balance of precipitation minus evapotranspiration (P-E), which includes the snowpack formation in winter as well as the snowmelt in spring. The daily runoff of 346 rivers was calculated for the time period 1970-2070. The annual average runoff and the day of the occurrence of spring maximum discharge were determined for the same period. The models predict a general increase of the annual runoff within the study area. On average, the increase varied from +0.9% to +10.3% between the bi-decadal period 1986-2005 and 2046-2065. In the latter bi-decadal period, the timing of the maximum discharge occurred between 1.1 and 16.3 days earlier in the year than during the reference period, due to the warmer air temperature in spring.

Résumé

Lambert, N., Chassé, J., Perrie, W., Long, Z., Guo, L. and Morrison, J. 2013. Projection of future river runoffs in Eastern Atlantic Canada from Global and Regional climate models. Can. Tech. Rep. Hydrogr. and Ocean. Sci. 288: viii + 34 p.

Les données de ruissellement provenant de trois modèles climatiques globaux (MCGs) ont été utilisées afin de déterminer le débit des rivières majeures débouchant dans l'atlantique du Nord-Ouest. Les MCGs (CanESM2, GFDL-ESM2M and MPI-ESM-LR) ont utilisé les scénarios d'émission des gaz à effet de serre (GES) provenant du GIEC AR5 (RCP 4.5 et RCP 8.5). Les modèles terrestres intégrés aux différents MCGs ont pu fournir l'information concernant l'écoulement de l'eau à la surface des bassins versants et ainsi, le débit des rivières a pu être déterminé. Les données provenant de deux modèles climatiques régionaux (MCRs), ont aussi été utilisées pour déterminer le débit de ces mêmes rivières. Les deux MCRs ont, quant à eux, utilisées les scénarios d'émission des GES provenant du GIEC AR4 (A1B et A2). Dans le cas des MCRs, un modèle hydrologique simple, basé sur la balance entre la précipitation et l'évapotranspiration (P-E) et sur la température de l'air, a permis de déterminer de ruissellement dans les bassins versant. Ce modèle hydrologique inclus l'accumulation de neige en hiver et le relâchement de cette eau au printemps, à l'arrivée de température au-dessus de zéro. Au total, les débits quotidiens de 346 rivières ont été calculés pour la période allant de 1970 à 2070. Pour la même période, le débit total annuel et le jour de l'année avec le débit maximum ont été déterminés pour chaque rivière.

Les modèles ont prédit une tendance générale vers la hausse des débits annuels des rivières dans toutes les principales régions analysées lors de cette étude. En moyenne, les débits ont augmenté de 0.9% à 10.3% entre les périodes 1986-2005 et 2046-2065. Au sein de la même période, le moment de l'année durant lequel le débit est à son maximum survient de 1.1 à 16.3 jours plus tôt en raison, entre autres, des températures plus clémentes au printemps.

1. Introduction

For the projection of marine ecosystem future conditions in Eastern Canada, it is important to know how global warming will affect the ocean conditions. More specifically, changes in the precipitation and evaporation regime can alter the runoff of the rivers flowing into the Atlantic. Different Global Climate Models (GCMs) developed within the CMIP5 project (http://www-pcmdi.llnl.gov/) have simulated the atmospheric conditions for the period 2006-2100. Although some GCMs predict an increase, others predict a decrease in the precipitation minus evaporation[1] (P-E) balance over the main watersheds in Canada (Chassé *et al*, 2013a). There is a tendency for an increasing trend over the Atlantic watershed in the ensemble mean of six GCMs but the Eastern Canada domain(Figure 1) contains many different rivers with their own watershed features and the general trend can't be applied over all of them.

The purpose of this analysis is to provide information on future freshwater runoff in Eastern Canada. Data from five different models were used to obtain statistics on the precipitation regime, i.e., three GCMs (CanESM2, GFDL-ESM2M and MPI-ESM-LR on RCP 4.5 and RCP 8.5 scenarios) and two regional models forced by CGCM 3.7 (DFO-CRCM with AR4-A1B SRES[2] scenario and Ouranos-CRCM with A2 SRES[2] scenario).

2. Models descriptions and methods

Data from two subtype of atmospheric models were used in the analysis: global climate models and regional climate models (RCMs). Those two subtypes of models were based on similar physic principles, but they were developed for different purposes. The GCMs calculate the atmospherics conditions on a large grid that covers the entire earth (Figure 2-a) while the RCMs use a sub-domain of the earth, which provides a better spatial resolution (Figure 2-b). In general, initial and lateral boundary conditions in a RCM are specified by a GCM that is compatible with its physics and type of grid.

2.1 Global climate models

Daily data were extracted from three GCMs, namely CanESM2, GFDL-ESM2M and MPI-ESM-LR. These GCMs are part of the CMIP5 multi-model ensemble (http://www-pcmdi.llnl.gov/). The future climate conditions (2006-2100) under different scenarios are available in the CMIP5 project and the scenarios RCP 4.5 and RCP 8.5 were selected for analysis. These projections were initialized from the end of a historical simulation (1850-2005) and thereafter forced by a medium anthropogenic greenhouse gas (GHG) emission scenario (RCP 4.5) and a high anthropogenic GHG emission scenario (RCP 8.5), as shown in the Figure 3.

Many variables can be extracted from the GCMs and we used the *runoff flux* to calculate the discharge of the rivers in Eastern Canada. The runoff flux corresponds to the water leaving the land portion of the grid cell and each GCM has its own land model to calculate these runoff fluxes. For example, CanESM2 uses the model CLASS (Canadian Land Surface Scheme, Verseghy 2000), a three soil layer model that includes snow production, the effect of vegetation on the precipitation/evaporation balance and the infiltration of water into porous soil. The runoff calculated by

[1] In the context of this study, the concept of evaporation include the evaporation from underlying surface and vegetation

[2] SRES : Special Report on Emissions Scenarios

CLASS (or the land surface model associate with each GCM) includes both surface and subsurface runoff. The subsurface runoff is composed of water drained through the bottom layer of the land model and the surface runoff is produced when the surface infiltration capacity is exceeded

We used the watershed grid shown in Figure 5 to determine the runoff of each river. To calculate the total runoff at a river's mouth, a delay proportional to the distance between the runoff grid cells and the mouth was given to the *runoff flux* of the land cells. This approach provided an approximation for the time required for a water parcel to flow to the ocean. However, due to the simplicity of the hydrologic model, it can give non-realistic results such as zero runoffs during the winter. Those runoffs do not really happen in rivers and for that reason they were considered as an artifact of the simulation. This model flaw vanishes as longer time scales (e.g. year) are considered. The timing of the spring freshwater pulse was calculated using a 7-day moving average of the simulated daily runoff; this approach smooths out the strong discharges and spread them over a few days without affecting the timing of the peak flow. The future trends were calculated with data from 1970 to 2070 and the future anomaly was calculated by comparing the difference (in percent) between the bi-decade 1985-2005 and the bi-decade 2046-2065.

2.2 Regional climate models

The Canadian Regional Climate Model, DFO implementation, (DFO-CRCM, Guo *et al*., 2013), was used to calculate precipitation, evaporation and temperature over Eastern Canada (the domain in shown in Figure 2-a). The DFO-CRCM has been used to downscale three members of the A1B AR4 scenario to derive the future atmospheric conditions. The three members were named M3, M4 and M5 and their downscaled results differ due to the use of slightly different initial conditions. The frequency of the output of DFO-CRCM is six hour and the simulations cover the period 1970 to 2070. DFO-CRCM uses an improved ocean model and the details can be found in Guo *et al*. (2013).

Similarly, the Ouranos RCM (Caya and Laprise, 1999) calculates the atmospheric variables over Canada and the data was extracted over a sub-domain shown in Figure 2-b. The output frequency is every three hours for two 33-years periods, the first one from 1968 to 2000 and the other from 2038 to 2070. The key difference between DFO-CRCM and Ouranos-CRCM is that the latter was forced with the SRES A2 emissions scenario which forecast a more pronounced global warming past the mid-century (2050) than the A1B scenario used in the DFO version of RCM.

River runoff was calculated using the simple hydrology model and near surface air temperature (*Ta*) and P-E fields from RCM. When surface air temperatures was above the freezing point (0°C), precipitation was assumed liquid and runoff was calculated directly from P-E. Below freezing temperatures, the variable P-E was converted into snow that accumulates on land. Subsequently, when *Ta* was greater than the freezing point, the accumulated snow pack was allowed to slowly melt and contribute to runoff. Similar as for the calculation of the GCM runoff, a delay proportional to the distance between the runoff grid cells and the river's mouth was added. The hydrology model was calibrated and validated using data from the National Center for Environment Prediction (NCEP**,** Kalnay *et al*.**, 1996**) as forcing fields (Figure 4). Non-realistic results could appear for the runoff calculated by the simple hydrology model such as negative values when evaporation is higher than precipitation. Those values are artifacts of the simulation due to the simplicity of the hydrologic model (no saturated soil, no release reservoirs etc.), but they should not affect too

Zones	Nb. Of rivers	Watershed area [km^2]
Quebec	**4**	**1054760**
Estu	**29**	**206178**
sGSL	**49**	**74710**
nGSL	**80**	**203921**
Estu+nGSL	**113**	**1464858**
GOM+SS	**76**	**209233**
SNS	**28**	**39940**
sLabrador	**75**	**258008**

Table 1. Numbers of rivers in each zone and the area of their watershed.

much the average runoff over extended periods of time (e.g. year). The occurrence of the spring discharge was also calculated using a 7-day moving average of the simulated daily runoffs. The future trends were calculated by using data from 1970 to 2070 for DFO-CRCM and over the two periods used by Ouranos-CRCM (1968 to 2000 and 2038 to 2070). The future anomaly was calculated by comparing the difference (in percent) between the bi-decade 1985-2005 and the bi-decade 2046-2065.

3. Results

Eight areas were defined in order to present the results of different models and projections: the St. Lawrence River including rivers in the Quebec City area (hereafter referred as *Quebec),* the St. Lawrence Estuary (*Estu*)*,* the southern Gulf of St. Lawrence (*sGSL*)*,* the northern Gulf of St. Lawrence (*nGSL*)*,* the combined estuary and northern gulf (*Estu+nGSL*[3])*,* the Gulf of Maine and Scotian Shelf (*GOM+SS*)*,* the southern Newfoundland Shelf (*SNS*) and the southern Labrador (*sLabrador*). The freshwater flow within a region was calculated by summing the runoff of rivers reaching each area shown in Figure 5.Table 1 shows the characteristics of the rivers leading into the different regions. Table 2 shows the average runoff over the entire study period for each of the areas shown in Figure 5. Table 3 shows the day when the maximum runoff occurs for each area. These results were obtained using the three GCMs and the two RCMs previously described.

Both type of models (global and regional) show similar runoffs for *Estu, nGSL, GOM+SS* and *sLabrador* but the results diverge for *Quebec, sGSL, Estu+nGSL* and *SNS*. In most areas the overall trend of runoff was positive and, for the global models, the increase was more pronounced for the scenario RCP 8.5 than RCP 4.5 (Table 2). The day of maximum runoff appears earlier in the global models than in the regional models for all regions and the time series standard deviation was greater for the GCMs. For all regions, the trends for the occurrence day of the maximum runoff were negative for both the GCMs and the RCMs meaning that the flood peaks will occur earlier within the year (Table 3).

3.1 Runoff in the Quebec zone

3.1.1 Global climate models

The runoffs produced by global models in the *Quebec* zone are shown in Figure 6. The monthly runoff varied from 0 to 38000 m³/s for models CanESM2 and MPI-ESM-LR and between 8000 and 38000 m³/s for the GFDL-ESM2M (Figure 6-a). The annual average runoff was between 8000 and 12000 m³/s with generally higher values for the MPI-ESM-LR model and correspondingly lower values for the CanESM2 model. Therefore, MPI-ESM-LR was closer to the 1970-2000 observed annual mean of 11800 m³/s. Except for the scenario RCP 4.5 in CanESM2, where the flow decreased over time, all models and scenarios predicted a future increase in runoff. The ensemble means were 10323 m³/s and 10344 m³/s for scenarios RCP 4.5 and RCP 8.5 respectively while the future trends were +5.5 m³/s/y. and +10.37 m³/s/y. (future anomaly of +0.9% and 1.8%).

As expected, the maximum daily discharge occurred in the spring with a varying intensity. Figure 6-c shows that the maximum discharge occurred around day 96 (i.e., day of the year, April 6), and the timing of peak flow shows a decrease (occur earlier) in the future as predicted by CanESM2 and GFDL-ESM2M models. Peak flows were shown to occur later within the year (in the future) when

[3] The *Estu+nGSL* zone contains these existing zones: *Estu, nGSL* and *Quebec.* The runoffs in this region are shown in the Figure 20 and Figure 21 but they will not be discussed in this paper.

using the MPI-ESM-LR model. Whether results showed an increase or decrease, the three models predicted a more pronounced slope (greater change) for the scenario RCP 8.5 than for the scenario RCP 4.5 for the timing of the maximum discharge.

3.1.2 Regional climate models

For the period 1970-2070, monthly runoff calculated by the regional models in the *Quebec* zone can reach values up to 100000 m^3/s (Figure 7-a). This high value was larger than currently observed flows and probably reflects a snowpack that was modeled to melt too fast in the spring and the underestimated evaporation over the great lakes in winter (there is no lake model in the RCMs). The time series for different scenarios of regional models show a low runoff for summer and winter months, slightly higher flows during the fall and maximum values during the spring. In terms of mean annual runoff (Figure 7-b), they varied between 11000 and 14800 m^3/s (ensemble mean of 13514 m^3/s) and no clear trend was present (ensemble mean trend of 1.76 $m^3/s/y$). Moreover, the inter-annual variability seemed quite high for all scenarios of the two models. Finally, the average runoff for the member M3 of DFO-CRCM was systematically lower than in the other simulations reflecting a relatively drier climate in member M3.

The day within the year when the maximum runoff occurs is shown in Figure 7-c. Maximum runoff generally occurs around the day 160 (June 10) for the model DFO-CRCM and around day 125 (May 5) for the model Ouranos-CRCM. The timing of the maximum runoff decreases at a rate between 0.16 (DFO-CRCM, M3) and 0.73 (Ouranos-CRCM) days per year. However, the period over which the trend was calculated was shorter for Ouranos-CRCM, which may explain in part the higher slope.

3.2 Runoff in the St. Lawrence Estuary (Estu) zone

3.2.1 Global climate models

Monthly runoffs calculated from the global models varied from 0 to 15000 m^3/s in the *Estu* zone (Figure 8-a). The freshwater flow in this zone had its lowest values during the winter months and highest values were observed in the spring. As shown in Figure 8-b, the annual runoff was about 3500 m^3/s for GFDL-ESM2M and CanESM2 and 4500 m^3/s for MPI-ESM-LR. An increasing trend was calculated for the runoff in most cases, except for the CanESM2 scenario RCP 4.5, where the future runoff was projected to decrease slightly. The ensemble means of the future anomaly was +3.8% and +9.6% for RCP 4.5 and RCP 8.5 respectively.

Figure 8-c shows that the maximum runoff occurred around the day 110 (April 20) for CanESM2 and MPI-ESM-LR and earlier for GFDL-ESM2M (day 90: March 31). The three global models predicted that the maximum will occur earlier in the year in the future, with a rate between -0.067 and -0.385 days per year over the length of the time series (ensemble mean rates of -0.16 and -0.2 d/y for RCP 4.5 and RCP 8.5 respectively). The decrease was more pronounced for the scenario RCP 8.5 than for the scenario RCP 4.5.

3.2.2 Regional climate models

In the *Estu* zone, the monthly runoff varied from 0 to 20000 m^3/s for the two regional models (Figure 9-a). The flow rate was calculated to be lower for the winter months and higher for the spring months. The ensemble mean annual runoff was 4340 m^3/s including the lower value for the scenario M3 (DFO-CRCM). Aside from the scenario 1968 (Ouranos-CRCM) which predicts a decrease (over the period 1968-2000), all other scenarios predicted an increase in the future annual runoff of about 6 $m^3/s/y$. (future anomaly of +10.3%).

The day with maximum runoff was around the day 155 (June 4) for the DFO-CRCM and around day 130 day (May 10) for the Ouranos-CRCM. This day tends, on average, occurred a little earlier in the year with an average rate of -0.166 d/y.

3.3 Runoff in southern Gulf of St. Lawrence (sGSL) zone

3.3.1 Global climate models

In the *sGSL* zone, forcing the hydrology model with GCMs lead to a monthly runoff ranging from 0 to 3000 m³/s (Figure 10-a) with maximum values during the spring months. However, important flow rates were also observed in the fall. The calculated annual runoff, averaging a value around 1100 m³/s, showed a decreasing trend for the CanESM2 and MPI-ESM-LR, but an increasing trend for GFDL-ESM2M, leading to small ensemble positive trends that were not statistically significant.

The time of the year when the runoff reached its maximum was around the day 68 (March 9) for GFDL-ESM2M and MPI-ESM-LR and around day 80 (March 21) for the model CanESM2 (Figure 10-c) leading to an ensemble mean centered on day 73 (March 14). The three global models predicted that the maximum runoff of the year will occur earlier in the future, with a negative ensemble trend around -0.2 d/y for both RCP 4.5 and RCP 8.5 scenarios.

3.3.2 Regional climate models

The river runoff in the *sGSL* zone is shown in Figure 11. The monthly runoff varied from 0 to 9000 m³/s with the maximum occurring during the spring months (Figure 11-a). The ensemble average runoff over a year was about 1507 m³/s and tended to increase slightly according to the RCMs (ensemble average trend of +0.95 m³/s/y and a future anomaly of +4.9%).

Calculations made with DFO-CRCM (A1B) showed a maximum runoff (Figure 11-c) occurring on day 140 (May 20) and data from Ouranos-CRCM (A2) showed that the day with the maximum runoff occurred earlier, on day 110 (April 20). Both models agreed that the maximum runoff predicted an earlier timing of the maximum runoff in the future.

3.4 Runoff in the northern Gulf of St. Lawrence (nGSL) zone

3.4.1 Global climate models

Figure 12 shows the total runoff calculated from the GCMs and flowing into the *nGSL*. The total runoff varied between 0 and 15000 m³/s with higher values in spring. The annual mean runoff trends were predicted to increase (Figure 12-b) with an ensemble rate of 3.6 m³/s/y. (RCP 4.5) and 5.9 m³/s/y. (RCP 8.5) for an average initial flow of around 3950 m³/s (future anomaly of +3.5% and 8.5%).

The maximum flow occured around day 100 (April 10) for MPI-ESM-LR and GFDL-ESM2M and around day 117 (April 27) for the CanESM2 (Figure 12-c). In the long term, the timing of the maximum runoff will most likely occur sooner with a calculated trend of -0.17 to -0.37 d/y.

3.4.2 Regional climate models

Figure 13 shows the runoff of various rivers calculated by the regional models in the *nGSL* zone where the monthly runoffs varied from 0 to 25000 m³/s. The annual runoffs shown in Figure 13-b show that the initial value of 4482 m³/s gradually increases for all modeled cases with an ensemble mean rate of 4.3 m³/s/y. (future anomaly of +5.0%).

The runoff maximum occurred in the spring months, specifically around day 155 (June 4) for the DFO-CRCM and day 135 (May 15) for the Ouranos-CRCM giving an ensemble mean centered on day 153 (Figure 13-c). The day of year for the timing of the maximum runoff was projected to decrease over the study period with a trend of -0.139 d/y.

3.5 Runoff in the Gulf of Maine and Scotian Shelf (GOM+SS) zone

3.5.1 Global climate models

The calculations made from the global models show that, in the *GOM+SS* zone, the monthly runoff can be around 1000 m³/s in the summer and up to 10000 m³/s in the spring (Figure 14-a). The discharge was strongest during day 66 (March 7) and the global models predicted that the maximum will occur sooner with an ensemble trend of -0.11 d/y. Surprisingly, GFDL-ESM2M and MPI-ESM-LR predicted that the trend will be less pronounced for the scenario RCP 8.5, even if this scenario is based on greater GHG emissions. Finally, the mean annual runoffs were different for the three global models: 2700 m³/s for CanESM2, 3100 m³/s for GRDF-ESM2M and 3300 m³/s for MPI-ESM-LR giving ensemble means of 3066 m³/s and 3085 m³/s for the two RCPs scenarios (Figure 14-b). The trends for the future were also different for each model: positive for CanESM2 and MPI-ESM-LR and negative for GFDL-ESM2M.

3.5.2 Regional climate models

The runoffs in the *GOM+*SS zone calculated by the two regional models are shown in the Figure 15. In that area, the monthly mean runoff ranged between 0 and 25000 m³/s with a maximum value observed in the spring. The ensemble mean annual runoff was around 4100 m³/s and there were no clear trends for the future projection (Figure 15-b).

The timing of maximum runoff occurred around day 130 (May 10) for the DFO-CRCM and around day 108 (April 18) for the Ouranos-CRCM with the ensemble mean centered on day 124 (Figure 15-c). The ensemble mean trend for the timing of the maximum runoff was negative at -0.26 d/y.

3.6 Runoff in the Southern Newfoundland Shelf (SNS) zone

3.6.1 Global climate models

The monthly runoffs in the *SNS* zone are shown in the Figure 16-a, and they were ranging between 100 m³/s and 1500 m³/s with lower flows in winter and summer and higher values in spring. The annual runoff was different for each of the global model: 310 m³/s for CanESM2 and 500 m³/s for GFDL-ESM2M and lead to the ensemble mean around 420 m³/s (Figure 16-b).

On average, each global model showed a different day for the occurrence of the maximum runoff (Figure 16-c): day 80 (Mar. 21) for CanESM2, day 51 (Feb. 20) for GFDL-ESM2M and day 68 for MPI-ESM-LR giving an ensemble mean centered on day 67 for each of the two RCPs scenarios. Unexpectedly, the GFDL-ESM2M model predicted that the maximum runoff will occur later in the future while the other models predicted that it will occur sooner. The ensemble trends were around 0.2 d/y for both RCPs scenarios.

3.6.2 Regional climate models

In the *SNS* zone, the monthly runoff calculated by the regional models varied between 0 m³/s in winter and around 5000 m³/s during spring (Figure 17-a) with an ensemble average flow of 1140 m³/s.

Figure 17-b shows that the annual runoffs were around 1100 m³/s and they seem to be stable in the future.

The day with the maximum runoff (Figure 17-c) occurred around day 135 (May 15) for the DFO-CRCM, but it occured much sooner with the Ouranos-CRCM (day 109 and day 84: April 19 and March 25). This gives an ensemble mean of 128 days for the occurrence of the maximum runoff. Except for the simulation 2038-2070 (Ouranos-CRCM), all the simulations predicted an earlier occurrence of the maximum runoff in the future.

3.7 Runoff in the Southern Labrador (sLabrador) zone

3.7.1 Global climate models

In Figure 18-a, the three global models showed that the monthly runoff varied from 0 to 20000 m³/s in the *sLabrador* zone with an ensemble average of 4900 m³/s in both RCP scenarios. Moreover, the annual runoff was projected to increase in the future: with an ensemble mean rate of 3.1 m³/s/y. in RCP 4.5 to 5.9 m³/s/y. in RCP 8.5 (Figure 18-b). On an average runoff of 4900 m³/s, this increase leads to future anomalies of +3.4% and +7.3%.

The maximum runoff occurs in the summer, and the minimum occurs in the winter. Due to the colder temperatures compared to other areas, the day with the maximum runoff occurred around day 125 (May 5), and the timing was slightly earlier for the MPI-ESM-LR and later for the CanESM2 (Figure 18-c). All models predicted an earlier spring discharge in the future, with a trend between -0.179 to -0.305 d/y (ensemble mean of -0.17 d/y).

3.7.2 Regional climate models

The monthly runoffs in the *sLabrador* zone, illustrated in the Figure 19-a, can reach up to 25000 m³/s during the spring discharge. The runoff has a very distinct annual cycle with a maximum in the summer and a minimum in the winter. The runoff was projected to increase significantly in the future with a rate varying from 2.34 m³/s/y. to 18.39 m³/s/y. (Figure 19-b). This represents a future anomaly of 5.2% of the average annual runoff.

Compare to the other zones, the air temperature over southern Labrador is colder, which then affects the day when the runoff is a maximum. Indeed, this higher runoff occurred around the 162th day (June 11) for the DFO-CRCM and around the 145th day (May 25) for the Ouranos-CRCM giving an ensemble mean centered on day 160 (Figure 19-c). Moreover, all the scenarios predicted that the maximum runoff will happen sooner in the future with a trend between -0.094 and -0.255 d/y (ensemble mean of -.13 d/y).

4. Discussion and conclusion

Based on the Global Climate Models (GCMs) and the Regional Climate Models (RCMs) outputs, two different methods were used to calculate the runoff of 346 rivers of eastern Canada. One method used the water drainage calculated by GCM land surface models. The other method used the balance between precipitation and evaporation (P-E) and air temperature to calculate the total runoff. This calculation included the accumulation of snow in winter and the production of snow melt water in spring. With these two different methods, future projections of the annual runoff were showing a projected increase of +0.9% to +10.3% between the bi-decade 1986-2005 and the bi-decade 2046-2065 depending on the sub-area considered. Over the same time interval, the timing of peak flow or peak runoff showed an earlier-in-the-year occurrence of 1.1 to 16.3 days. Similarly, Frigon *et al.*

(2010) showed an increase between 9±6% and 33±14% of the simulated surface runoff (P-E) over 21 rivers basins in Quebec. In their study, the increase was greater in the northen part of Quebec than in the southern part. They explained this phenomenon by the overall rise in precipitation and the more important increase in evaporation in the southern part of the domain. Huziy *et al.* (2012) found similar results with an important increase of the stream flow during spring in the northern part of Quebec and an increase, mostly in fall, in the southern part. For the timing of the maximum runoff in spring, a study carried out over the Manicouagan river basin (above the Manic 5 dam) located in central Quebec found a decrease of 6 to 22 days of the maximum runoff over the 2025−2085 period (Chen *et al.* 2012).

Comparing results from our two methods, both approaches gives similar future trends for the annual runoff (Table 2) and some of the difference may be attributed to the difference in grid cell sizes between the GCMs and the RCMs (Figure 2). The major difference in results between the two methods is the variation of the monthly runoff. The method used with the RCMs provided a spring discharge greater than the method used by the GCMs. Moreover, the days with the maximum runoff occurred later with the RCM method, even if they agreed on the future trend. The peak maximum runoff occurs earlier in GCMs probably due to warmer land surface temperature near the coasts than in RCMs; this lead to a greater snow pack accumulation during winter in RCMs and thus a delayed spring discharge. Di Luca *et al.* (2011) showed in their study that RCMs give general better results for short temporal scale processes. The important spatial and temporal temperature gradient present in spring time may be better represented in RCMs than in the GCMs. However, the simulations giving the higher runoff were downscaled from the A1B and A2 scenarios which tend to predict wetter conditions than RCP 4.5 and RCP 8.5 scenarios over Canada. Extreme precipitation events may not be well simulated by the GCMs, but they are more significant in summer and in fall (Monette *et al.*, 2012). DFO-CRCM also showed a later occurrence of the maximum runoff than Ouranos-CRCM due to an improved representation of the SST in DFO-CRCM. Although the use of two different land surface models might be expected to contribute to the differences between RCMs and GCMs, a surface runoff sensibility study made for the St. Lawrence basin (Music and Caya, 2009) concluded that modifications in the land models did not significantly affect the global runoff in this region.

The goal of this report was to quantify possible future river runoffs in Eastern Canada using available climate change scenarios. It was not to provide exact absolute values for runoff, but rather to provide relative information about the possible future change. In that sense, results presented here should not be used without an appropriate scaling to match historical observed conditions.

5. Acknowledgements

We acknowledge the World Climate Research Programme's Working Group on Coupled Modelling, which is responsible for CMIP, and we thank the climate modeling groups for producing and making available their model output. We are also thankful to the OURANOS consortium for providing the precipitation and air temperature data from their RCM. We acknowledge the NOAA for the *NCEP Reanalysis data.* Finally, we thank Dave Brickman and Daniel Caissie for their comments on an earlier version of this document.

6. References

Caya, D., and R. Laprise. 1999. A Semi-Implicit Semi-Lagrangian Regional Climate Model: The Canadian RCM. *Mon. Wea. Rev*., 127, 341-362.

Chassé, J., Lambert, N. and Lavoie, D. 2013a. Precipitation, Evaporation and Freshwater Flux over Canada from six Global Climate Models. Can. Tech. Rep. Hydrogr. Ocean Sci. 287: viii + 47 p.

Chassé, J., W. Perrie, Z. Long, D. Brickman, L. Guo and N. Lambert. 2013b. Regional atmosphere-ocean-ice climate downscaling results for the Gulf of St. Lawrence using the DFO Regional Climate Downscaling System. *Can. Tech. Rep. Hydrogr. Ocean Sci. (in preparation)*.

Chassé, J., Lambert N. and Lavoie, D. 2013. Precipitation, Evaporation and Freshwater Flux over Canada from six Global Climate Models. Can. Tech. Rep. Hydrogr. Ocean Sci. 287: viii + 47 pp.

Chen, J., F. P. Brissette, R. Leconte. 2012. Downscaling of weather generator parameters to quantify hydrological impacts of climate change. Clim Res, 51: 185–200, doi: 10.3354/cr01062.

Di Luca, A., R. De Elìa, R. Laprise. 2012. Potential for added value in precipitation simulated by high-resolution nested Regional Climate Models and observations, *Clim Dyn*, 38, 1229–1247, doi: 10.1007/s00382-011-1068-3.

Frigon, A., B. Music, M. Slivitzky. 2010. Sensitivity of runoff and projected changes in runoff over Quebec to the update interval of lateral boundary conditions in the Canadian RCM, *Meteorologische Zeitschrift*, 19: 3, 225-236, doi: 10.1127/0941-2948/2010/0453.

Guo,L. W. Perrie, Z. Long, J. Chassé, Y. Zhang and A. Huang. 2012. Dynamical downscaling over the Gulf of St. Lawrence using the Canadian Regional Climate Model. *Atmosphere-ocean* (in press).

Huziy, O., L. Sushama, M. N. Khaliq, R. Laprise, B. Lehner, R. Roy. 2013. Analysis of streamflow characteristics over Northeastern Canada in a changing climate, *Clim Dyn*, 40, 1879–1901, doi : 10.1007/s00382-012-1406-0.

Kalnay, E., and Coauthors. 1996: The NCEP/NCAR 40-Year Reanalysis Project. *Bull. Amer. Meteor. Soc.*, 77, 437–471.

Monette, A., L. Sushama, M. N. Khaliq, R. Laprise, R. Roy. 2012. Projected changes to precipitation extremes for northeast Canadian watersheds using a multi-RCM ensemble, *J. Geophys. Res*., 117, D13106, doi:10.1029/2012JD017543.

Music, B., D. Caya. 2009. Investigation of the Sensitivity of Water Cycle Components Simulated by the Canadian Regional Climate Model to the Land Surface Parameterization, the Lateral Boundary Data, and the Internal Variability, *J. of Hydrometeorology*, doi : 10.1175/2008JHM979.1.

Music, B., A. Frigon, M. Slivitzky, A. Musy, D. Caya, R. Roy. 2009. Runoff modelling within the Canadian Regional Climate Model (CRCM): analysis over the Quebec/Labrador watersheds, (Proc. of Symposium HS.2 at the Joint IAHS & IAH Convention, Hyderabad, India, September 2009). International Association of Hydrological Sciences (IAHS) Red Book Series Publ. 333, 183-194.

Verseghy (2000), The Canadian land surface scheme (CLASS): Its history and future, *Atmoshere-Ocean*, 38:1, 1-13.

7. Tables and Figures

Zone	Global models and scenarios		Mean	STD	Trend	Future anomaly
			m^3/s	m^3/s	$[m^3/s]/y$	%
Quebec	CanESM2	RCP 4.5	8683	1492.0	-4.493	-1.5 %
	GFDL-ESM2M	RCP 4.5	10393	1334.3	+9.987	+4.8 %
	MPI-ESM-LR	RCP 4.5	11894	2535.1	+11.017	-0.6 %
	All models	**RCP 4.5**	**10323**	**1118.6**	**+5.504**	**+0.9 %**
	CanESM2	RCP 8.5	8903	1657.4	+9.223	+6.2 %
	GFDL-ESM2M	RCP 8.5	10184	1286.4	+6.880	-1.3 %
	MPI-ESM-LR	RCP 8.5	11946	2756.6	+14.997	+1.1 %
	All models	**RCP 8.5**	**10344**	**1114.3**	**+10.366**	**+1.8 %**
Estu	CanESM2	RCP 4.5	3531	587.3	-0.210	+2.2 %
	GFDL-ESM2M	RCP 4.5	3607	553.0	+6.259	+7.6 %
	MPI-ESM-LR	RCP 4.5	4457	748.6	+4.501	+1.8 %
	All models	**RCP 4.5**	**3865**	**376.7**	**+3.517**	**+3.8 %**
	CanESM2	RCP 8.5	3595	675.6	+6.185	+17.6 %
	GFDL-ESM2M	RCP 8.5	3563	484.0	+5.042	+4.7 %
	MPI-ESM-LR	RCP 8.5	4532	741.7	+4.715	+7.5 %
	All models	**RCP 8.5**	**3897**	**377.1**	**+5.314**	**+9.6 %**
sGSL	CanESM2	RCP 4.5	1151	211.6	+0.685	+7.8 %
	GFDL-ESM2M	RCP 4.5	1092	152.9	-0.427	-6.5 %
	MPI-ESM-LR	RCP 4.5	1098	222.9	+0.631	+5.3 %
	All models	**RCP 4.5**	**1114**	**125.3**	**+0.297**	**+2.2 %**
	CanESM2	RCP 8.5	1181	237.6	+2.474	+21.5 %
	GFDL-ESM2M	RCP 8.5	1105	126.8	-0.592	-1.9 %
	MPI-ESM-LR	RCP 8.5	1079	200.8	+1.039	+5.1 %
	All models	**RCP 8.5**	**1122**	**111.3**	**+0.974**	**+8.2 %**
nGSL	CanESM2	RCP 4.5	4094	565.5	+1.660	+6.9 %
	GFDL-ESM2M	RCP 4.5	3866	545.0	+3.350	+0.2 %
	MPI-ESM-LR	RCP 4.5	3865	601.5	+5.725	+3.4 %
	All models	**RCP 4.5**	**3941**	**341.1**	**+3.578**	**+3.5 %**
	CanESM2	RCP 8.5	4149	611.6	+7.298	+18.1 %
	GFDL-ESM2M	RCP 8.5	3882	463.0	+3.397	+2.2 %
	MPI-ESM-LR	RCP 8.5	3899	578.1	+7.105	+5.2 %
	All models	**RCP 8.5**	**3976**	**372.2**	**+5.933**	**+8.5 %**

Regional models and scenarios		Mean	STD	Trend	Future anomaly
		m^3/s	m^3/s	$[m^3/s]/y$	%
D-CRCM	M3	11188	2337.9	+5.671	+11.6 %
D-CRCM	M4	14409	2387.4	+0.152	+2.3 %
D-CRCM	M5	14340	2780.9	+1.457	-8.2 %
O-CRCM	1968	14800	2156.3	-70.780	+0.0 %
O-CRCM	2038	14676	2219.5	+30.708	+6.7 %
All models		**13514**	**1402.6**	**+1.757**	**+2.6 %**
D-CRCM	M3	4010	617.2	+7.617	+17.2 %
D-CRCM	M4	4585	624.8	+5.057	+10.6 %
D-CRCM	M5	4551	616.9	+6.306	+6.3 %
O-CRCM	1968	4037	497.1	-6.922	+0.0 %
O-CRCM	2038	4288	551.6	+7.832	+9.0 %
All models		**4340**	**385.3**	**+5.744**	**+10.3 %**
D-CRCM	M3	1385	209.6	+1.948	+9.9 %
D-CRCM	M4	1551	226.2	+0.870	+2.7 %
D-CRCM	M5	1533	242.7	+1.779	+6.7 %
O-CRCM	1968	1645	261.1	-6.261	+0.0 %
O-CRCM	2038	1566	219.1	+2.203	-0.2 %
All models		**1507**	**144.2**	**+0.948**	**+4.9 %**
D-CRCM	M3	4120	547.9	+5.865	+8.3 %
D-CRCM	M4	4637	562.9	+4.256	+2.6 %
D-CRCM	M5	4682	635.8	+3.913	+6.9 %
O-CRCM	1968	4438	656.9	+7.736	+0.0 %
O-CRCM	2038	4586	644.7	+5.115	+1.7 %
All models		**4482**	**367.1**	**+4.278**	**+5.0 %**

Table 2. Table of the mean runoff calculated for the eight zones using three global climate models: CanESM2, GFDL-ESM2M and MPI-ESM-LR for scenarios RCP 4.5 and RCP 8.5 and two regional climate models: DFO-CRCM (scenario A1B, members M3, M4 and M5) and Ouranos-CRCM (scenario A2, periods 1968-2000 and 2038-2070). The mean, the standard deviation and the trend was calculated using the annual means over 100 years (except for Ouranos-CRCM; the time period was 33 years). The future anomaly was calculated with the difference (in percent) between the means of the bi-decade 1985-2005 and the bi-decade 2046-2065.

Zones	Global models and scenarios		Mean	STD	Trend	Future anomaly
			m^3/s	m^3/s	$[m^3/s]/yr.$	%
ESTU+nGSL	CanESM2	RCP 4.5	16308	2085.5	-3.043	+1.3 %
	GFDL-ESM2M	RCP 4.5	17866	2069.7	+19.596	+4.4 %
	MPI-ESM-LR	RCP 4.5	20216	3325.4	+21.242	+0.7 %
	All models	**RCP 4.5**	**18130**	**1516.6**	**+12.598**	**+2.0 %**
	CanESM2	RCP 8.5	16646	2419.4	+22.706	+11.4 %
	GFDL-ESM2M	RCP 8.5	17629	1816.6	+15.319	+0.7 %
	MPI-ESM-LR	RCP 8.5	20377	3475.8	+26.817	+3.3 %
	All models	**RCP 8.5**	**18217**	**1516.8**	**+21.614**	**+4.9 %**
GOM+SS	CanESM2	RCP 4.5	2708	492.4	+0.918	+4.4 %
	GFDL-ESM2M	RCP 4.5	3363	417.8	-1.671	-2.8 %
	MPI-ESM-LR	RCP 4.5	3125	654.3	+1.913	-0.0 %
	All models	**RCP 4.5**	**3066**	**337.3**	**+0.387**	**+0.3 %**
	CanESM2	RCP 8.5	2792	630.8	+5.426	+17.7 %
	GFDL-ESM2M	RCP 8.5	3384	411.5	-1.814	-1.2%
	MPI-ESM-LR	RCP 8.5	3078	597.5	+2.209	+1.8 %
	All models	**RCP 8.5**	**3085**	**308.3**	**+1.940**	**+5.4 %**
SNS	CanESM2	RCP 4.5	308	58.5	-0.247	+1.8 %
	GFDL-ESM2M	RCP 4.5	496	79.1	+0.187	-3.1 %
	MPI-ESM-LR	RCP 4.5	457	79.4	+0.520	+14.4 %
	All models	**RCP 4.5**	**421**	**43.9**	**+0.153**	**+4.4 %**
	CanESM2	RCP 8.5	314	58.4	+0.028	+5.3 %
	GFDL-ESM2M	RCP 8.5	509	81.3	+0.615	+10.2 %
	MPI-ESM-LR	RCP 8.5	455	76.0	+0.630	+8.6 %
	All models	**RCP 8.5**	**426**	**43.3**	**+0.424**	**+8.4 %**
sLabrador	CanESM2	RCP 4.5	5299	599.1	-0.109	+1.3 %
	GFDL-ESM2M	RCP 4.5	4600	528.7	+3.384	+3.2 %
	MPI-ESM-LR	RCP 4.5	4727	655.2	+6.050	+6.0 %
	All models	**RCP 4.5**	**4875**	**355.6**	**+3.108**	**+3.4 %**
	CanESM2	RCP 8.5	5392	642.4	+6.092	+10.1 %
	GFDL-ESM2M	RCP 8.5	4594	517.6	+4.047	+4.9 %
	MPI-ESM-LR	RCP 8.5	4785	634.5	+7.659	+6.6 %
	All models	**RCP 8.5**	**4923**	**404.7**	**+5.932**	**+7.3 %**

Regional models and scenarios		Mean	STD	Trend	Future anomaly
		m^3/s	m^3/s	$[m^3/s]/yr.$	%
D-CRCM	M3	19318	2763.7	+19.153	+12.0 %
D-CRCM	M4	23631	3013.1	+9.465	+3.9 %
D-CRCM	M5	23574	3342.3	+11.676	-2.7 %
O-CRCM	1968	23275	2839.9	-69.966	+0.0 %
O-CRCM	2038	23551	2906.9	+43.655	+6.1 %
All models		**22335**	**1868.0**	**+11.778**	**+4.5 %**
D-CRCM	M3	3687	547.0	+4.655	+11.0 %
D-CRCM	M4	4221	649.1	-1.457	-3.1 %
D-CRCM	M5	4106	650.8	+3.337	+4.4 %
O-CRCM	1968	4407	697.6	-18.360	+0.0 %
O-CRCM	2038	4297	679.3	-1.983	+2.6 %
All models		**4059**	**398.9**	**+1.270**	**+3.8 %**
D-CRCM	M3	1071	126.0	+0.496	+4.4 %
D-CRCM	M4	1189	145.5	+0.802	-2.0 %
D-CRCM	M5	1203	154.2	+0.671	+5.3 %
O-CRCM	1968	1047	142.8	-0.769	+0.0 %
O-CRCM	2038	1071	144.8	-0.522	+1.9 %
All models		**1139**	**90.6**	**+0.648**	**+2.0 %**
D-CRCM	M3	3808	501.7	+4.827	+5.1 %
D-CRCM	M4	4374	492.8	+2.342	-0.7 %
D-CRCM	M5	4382	585.3	+2.365	+7.9 %
O-CRCM	1968	5111	666.3	+18.388	+0.0 %
O-CRCM	2038	5458	544.5	+8.413	+2.9 %
All models		**4357**	**376.5**	**+3.823**	**+5.2 %**

Table 2. … (continued)…

Zones	Global models and scenarios		Mean	STD	Trend	Future anomaly
			Day	Day	Day/y	Days
Quebec	CanESM2	RCP 4.5	103	23.6	-0.190	-16.5
	GFDL-ESM2M	RCP 4.5	101	28.5	-0.209	-5.1
	MPI-ESM-LR	RCP 4.5	86	31.5	+0.108	+9.2
	All models	**RCP 4.5**	**96**	**17.3**	**-0.097**	**-4.0**
	CanESM2	RCP 8.5	103	25.8	-0.208	-24.8
	GFDL-ESM2M	RCP 8.5	102	31.5	-0.308	-13.9
	MPI-ESM-LR	RCP 8.5	87	32.6	+0.175	+9.9
	All models	**RCP 8.5**	**97**	**17.7**	**-0.114**	**-9.4**
Estu	CanESM2	RCP 4.5	107	25.6	-0.296	-18.8
	GFDL-ESM2M	RCP 4.5	114	30.3	-0.067	+0.4
	MPI-ESM-LR	RCP 4.5	90	29.0	-0.116	+3.8
	All models	**RCP 4.5**	**104**	**19.3**	**-0.160**	**-4.6**
	CanESM2	RCP 8.5	104	27.5	-0.385	-23.4
	GFDL-ESM2M	RCP 8.5	115	29.1	-0.138	-5.0
	MPI-ESM-LR	RCP 8.5	89	31.6	-0.079	+1.4
	All models	**RCP 8.5**	**103**	**17.0**	**-0.201**	**-8.6**
sGSL	CanESM2	RCP 4.5	81	33.4	-0.332	-38.4
	GFDL-ESM2M	RCP 4.5	69	31.1	-0.174	+4.3
	MPI-ESM-LR	RCP 4.5	68	32.4	-0.070	-4.2
	All models	**RCP 4.5**	**73**	**19.4**	**-0.192**	**-16.1**
	CanESM2	RCP 8.5	79	30.4	-0.409	-22.7
	GFDL-ESM2M	RCP 8.5	71	32.1	-0.225	-2.8
	MPI-ESM-LR	RCP 8.5	64	25.9	-0.061	-8.9
	All models	**RCP 8.5**	**72**	**18.0**	**-0.232**	**-14.5**
nGSL	CanESM2	RCP 4.5	120	27.2	-0.263	-26.1
	GFDL-ESM2M	RCP 4.5	99	34.7	-0.323	-19.9
	MPI-ESM-LR	RCP 4.5	101	29.6	-0.173	-2.7
	All models	**RCP 4.5**	**107**	**19.2**	**-0.253**	**-14.1**
	CanESM2	RCP 8.5	116	25.9	-0.365	-19.1
	GFDL-ESM2M	RCP 8.5	99	35.5	-0.329	-20.8
	MPI-ESM-LR	RCP 8.5	95	34.1	-0.244	-14.3
	All models	**RCP 8.5**	**103**	**19.4**	**-0.313**	**-15.7**

Regional models and scenarios		Mean	STD	Trend	Future anomaly
		Day	Day	Day/y	Days
D-CRCM	M3	158	11.8	-0.155	-11.3
D-CRCM	M4	162	12.8	-0.163	-12.8
D-CRCM	M5	161	11.5	-0.181	-6.3
O-CRCM	1968	130	10.3	-0.413	+0.0
O-CRCM	2038	120	30.9	-0.728	-7.0
All models		**155**	**9.4**	**-0.169**	**-7.1**
D-CRCM	M3	151	11.3	-0.170	-11.6
D-CRCM	M4	156	11.2	-0.119	-6.4
D-CRCM	M5	155	10.4	-0.122	-7.5
O-CRCM	1968	135	13.4	-0.212	+0.0
O-CRCM	2038	119	22.8	-0.203	-16.0
All models		**150**	**8.5**	**-0.166**	**-7.7**
D-CRCM	M3	136	11.5	-0.116	-6.9
D-CRCM	M4	140	10.4	-0.127	-8.1
D-CRCM	M5	137	10.7	-0.053	-0.2
O-CRCM	1968	120	14.8	-0.434	+0.0
O-CRCM	2038	95	32.7	-1.376	-23.9
All models		**133**	**9.5**	**-0.175**	**-8.0**
D-CRCM	M3	154	9.8	-0.130	-6.6
D-CRCM	M4	158	10.4	-0.125	-11.0
D-CRCM	M5	157	9.5	-0.098	-6.1
O-CRCM	1968	140	16.9	-0.449	+0.0
O-CRCM	2038	130	17.8	-0.498	-7.2
All models		**153**	**7.3**	**-0.139**	**-5.6**

Table 3. Table of the day with the maximum runoff calculated for the eight zones by using three global climate models: CanESM2, GFDL-ESM2M and MPI-ESM-LR for scenarios RCP 4.5 and RCP 8.5 and two regional climate models: DFO-CRCM (scenario A1B, members M3, M4 and M5) and Ouranos-CRCM (scenario A2, periods 1968-2000 and 2038-2070). The mean, the standard deviation and the trend was calculated using the annual means over 100 years (except for Ouranos-CRCM; the time period was 33 years). The future anomaly was calculated as the difference (in percent) between the means of the bi-decade 1985-2005 and the bi-decade 2046-2065.

Zones	Global models and scenarios		Mean	STD	Trend	Future anomaly	Regional models and scenarios		Mean	STD	Trend	Future anomaly
			Day	Day	Day/y	Days			Day	Day	Day/y	%
ESTU+nGSL	CanESM2	RCP 4.5	109	21.8	-0.266	-15.8	D-CRCM	M3	156	11.1	-0.178	-12.9
	GFDL-ESM2M	RCP 4.5	104	32.6	-0.159	+9.2	D-CRCM	M4	162	10.6	-0.142	-9.8
	MPI-ESM-LR	RCP 4.5	91	25.4	-0.043	+3.2	D-CRCM	M5	160	10.6	-0.143	-5.1
	All models	**RCP 4.5**	**101**	**16.6**	**-0.156**	**-1.1**						
	CanESM2	RCP 8.5	106	26.3	-0.387	-15.1	O-CRCM	1968	134	8.5	-0.257	+0.0
	GFDL-ESM2M	RCP 8.5	103	32.1	-0.219	+2.9	O-CRCM	2038	118	24.5	-0.320	-16.5
	MPI-ESM-LR	RCP 8.5	90	28.5	-0.050	-2.5						
	All models	**RCP 8.5**	**100**	**17.1**	**-0.219**	**-4.8**	**All models**		**154**	**9.1**	**-0.176**	**-8.0**
GOM+SS	CanESM2	RCP 4.5	77	33.0	-0.202	-12.7	D-CRCM	M3	129	19.3	-0.244	-11.8
	GFDL-ESM2M	RCP 4.5	61	25.6	-0.077	+1.0	D-CRCM	M4	132	16.4	-0.231	-8.7
	MPI-ESM-LR	RCP 4.5	63	40.1	-0.189	-10.1	D-CRCM	M5	131	13.5	-0.165	-3.9
	All models	**RCP 4.5**	**67**	**19.1**	**-0.156**	**-10.7**						
	CanESM2	RCP 8.5	72	30.9	-0.290	-22.8	O-CRCM	1968	109	30.2	-0.769	+0.0
	GFDL-ESM2M	RCP 8.5	62	29.8	-0.016	-3.4	O-CRCM	2038	83	36.2	-0.635	-26.4
	MPI-ESM-LR	RCP 8.5	66	31.9	-0.031	-7.0						
	All models	**RCP 8.5**	**66**	**17.7**	**-0.112**	**-16.3**	**All models**		**125**	**13.0**	**-0.263**	**-10.9**
SNS	CanESM2	RCP 4.5	80	37.7	-0.402	-32.1	D-CRCM	M3	133	13.5	-0.186	-11.4
	GFDL-ESM2M	RCP 4.5	53	23.8	+0.053	+7.4	D-CRCM	M4	135	17.6	-0.273	-15.1
	MPI-ESM-LR	RCP 4.5	70	46.6	-0.199	-14.2	D-CRCM	M5	135	13.4	-0.173	-17.5
	All models	**RCP 4.5**	**67**	**21.9**	**-0.183**	**-17.0**						
	CanESM2	RCP 8.5	82	38.1	-0.336	-34.6	O-CRCM	1968	109	31.4	-1.497	+0.0
	GFDL-ESM2M	RCP 8.5	50	24.3	+0.032	+2.6	O-CRCM	2038	84	34.0	+0.511	-4.2
	MPI-ESM-LR	RCP 8.5	68	44.0	-0.084	-3.5						
	All models	**RCP 8.5**	**67**	**18.3**	**-0.129**	**-15.5**	**All models**		**129**	**13.0**	**-0.247**	**-10.9**
sLabrador	CanESM2	RCP 4.5	132	19.1	-0.161	-16.6	D-CRCM	M3	161	12.9	-0.160	-8.1
	GFDL-ESM2M	RCP 4.5	124	30.3	-0.222	-17.9	D-CRCM	M4	166	12.1	-0.160	-13.5
	MPI-ESM-LR	RCP 4.5	121	16.5	-0.134	-0.6	D-CRCM	M5	162	11.7	-0.094	-4.2
	All models	**RCP 4.5**	**125**	**14.9**	**-0.172**	**-8.9**						
	CanESM2	RCP 8.5	134	18.7	-0.179	-7.7	O-CRCM	1968	148	15.4	+0.139	+0.0
	GFDL-ESM2M	RCP 8.5	129	26.6	-0.190	-17.8	O-CRCM	2038	143	17.7	-0.255	-6.9
	MPI-ESM-LR	RCP 8.5	114	22.4	-0.305	-18.7						
	All models	**RCP 8.5**	**125**	**14.1**	**-0.225**	**-11.2**	**All models**		**160**	**8.3**	**-0.128**	**-5.5**

Table 3. (continued)…

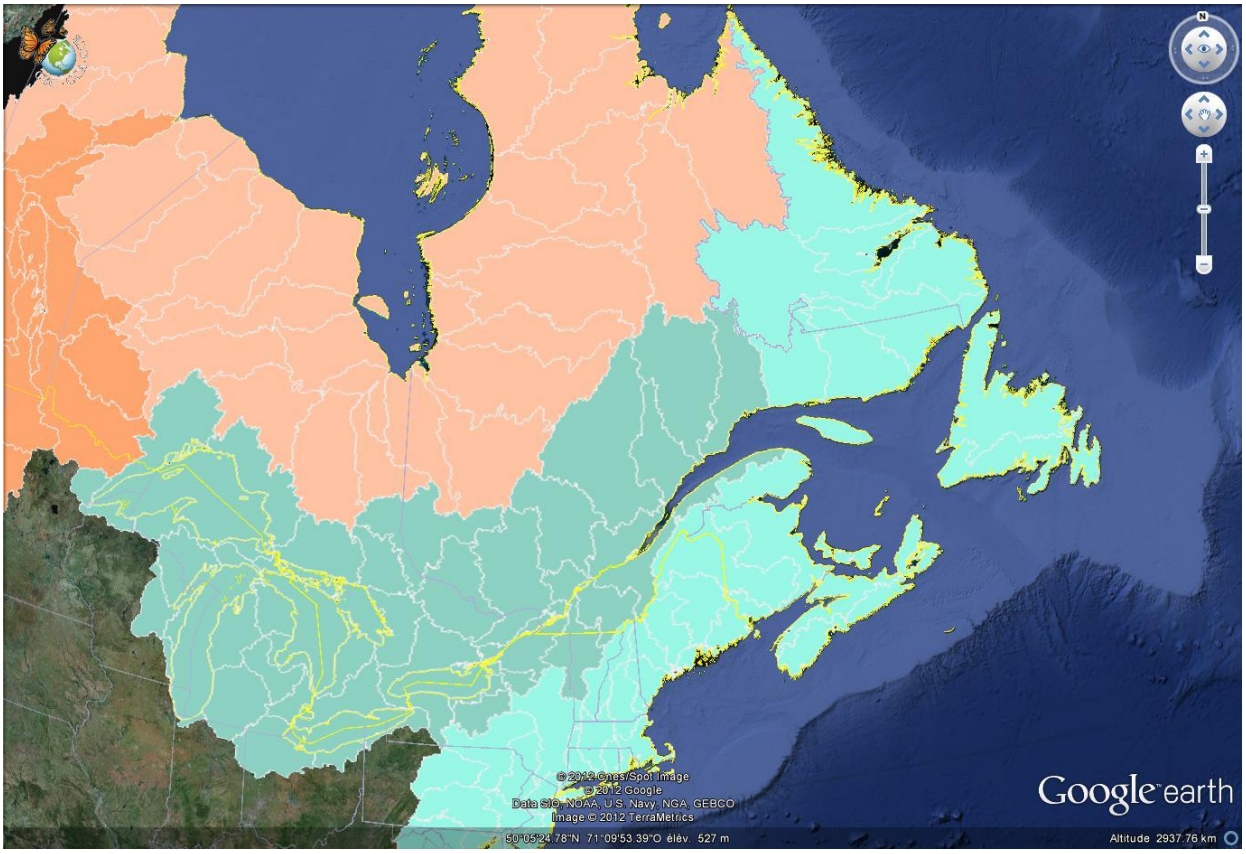

Figure 1. Map of the Atlantic watershed (green) and the Hudson Bay watershed (orange). The lines limit the major river's watershed. Image was generated by Google Earth and the location of the watershed comes from the Commission for Environmental Cooperation (www.cec.org).

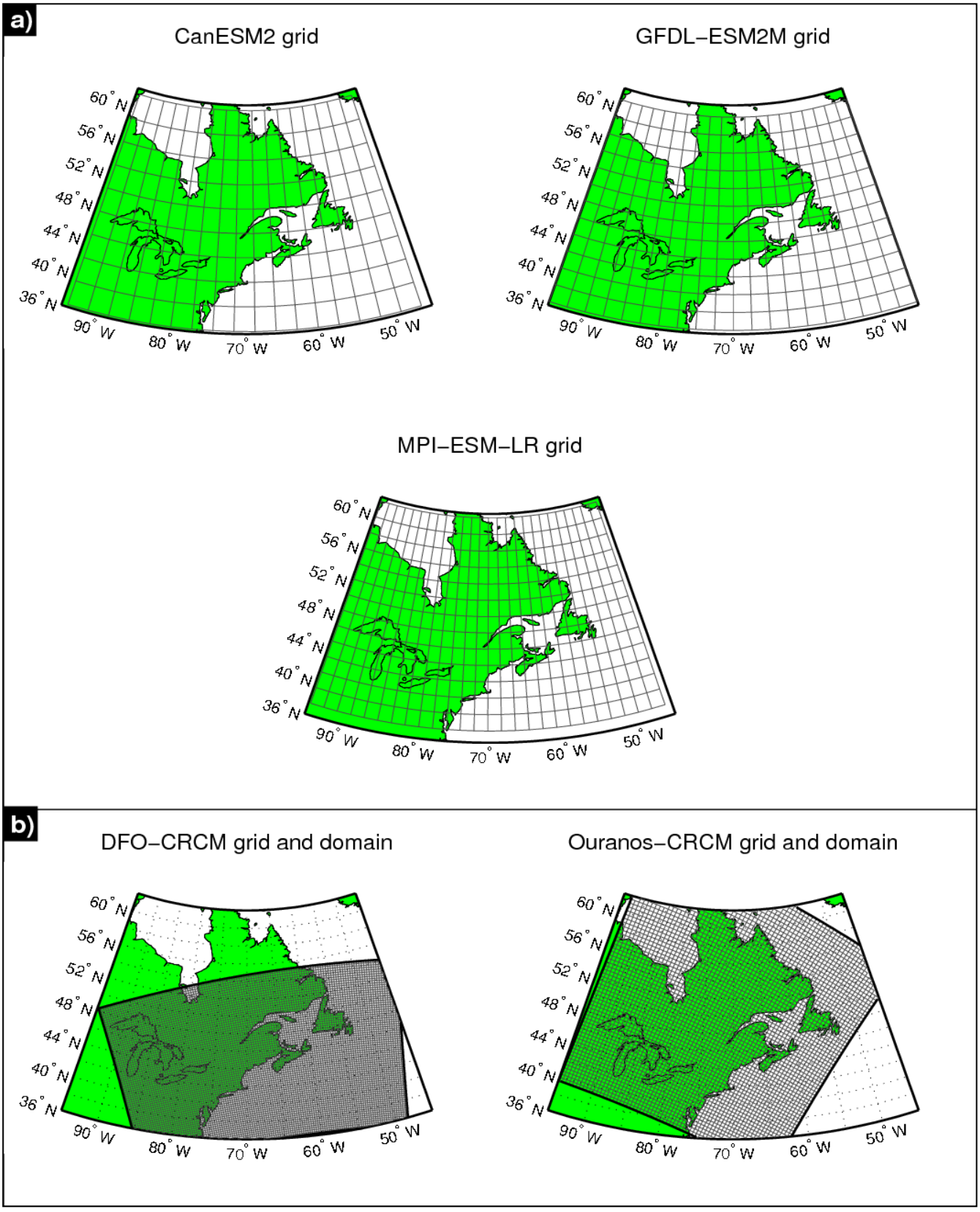

Figure 2. a) Grid resolution of the global models CanESM2, GFDL-ESM2M and MPI-ESM-LR. b) Grid resolution of the regional climate models DFO-CRCM and Ouranos-CRCM and the sub domains covered by the simulations.

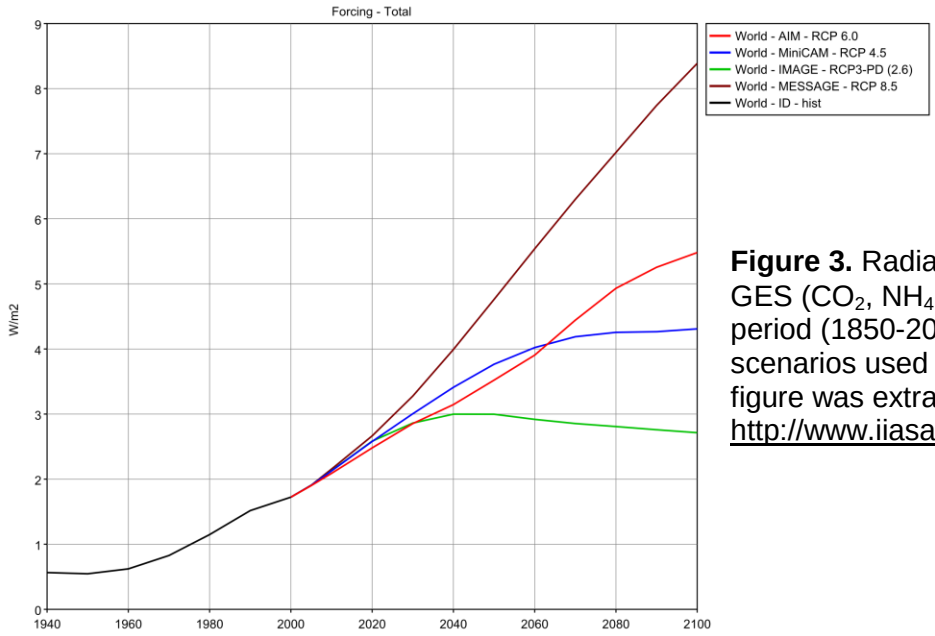

Figure 3. Radiative forcing induced by the GES (CO_2, NH_4, N_2O etc.) for the historical period (1850-2005) and the projection scenarios used by the CMIP5 project. This figure was extract from web site http://www.iiasa.ac.at/web-apps/tnt/RcpDb/.

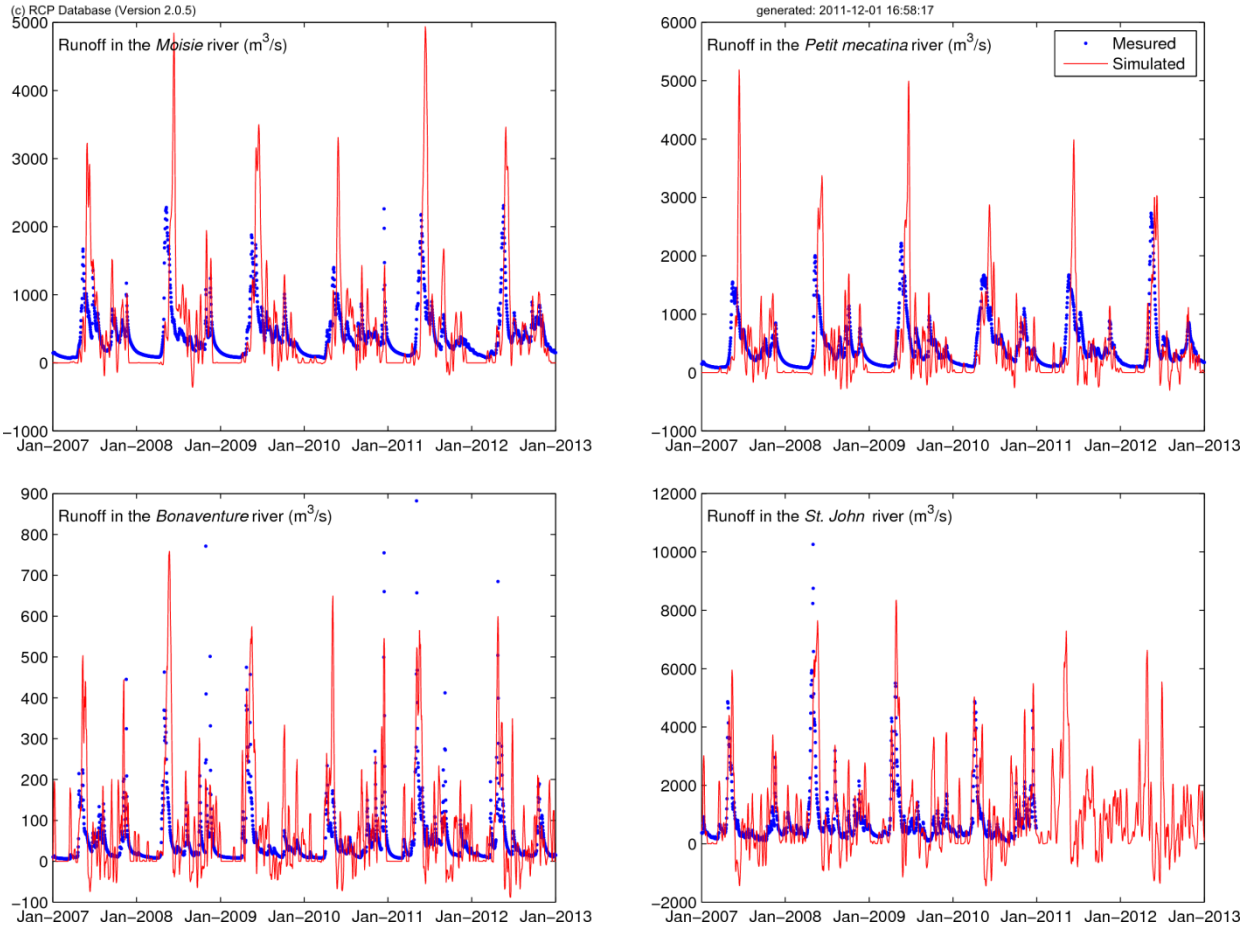

Figure 4. Example of model skill; Time series of the daily runoff of four rivers measured by hydrologic stations and the daily runoff calculated by the simple hydrologic model fed by precipitation, evaporation and temperature of the NCEP/NCAR reanalysis project (Kalnay et al., 1996).

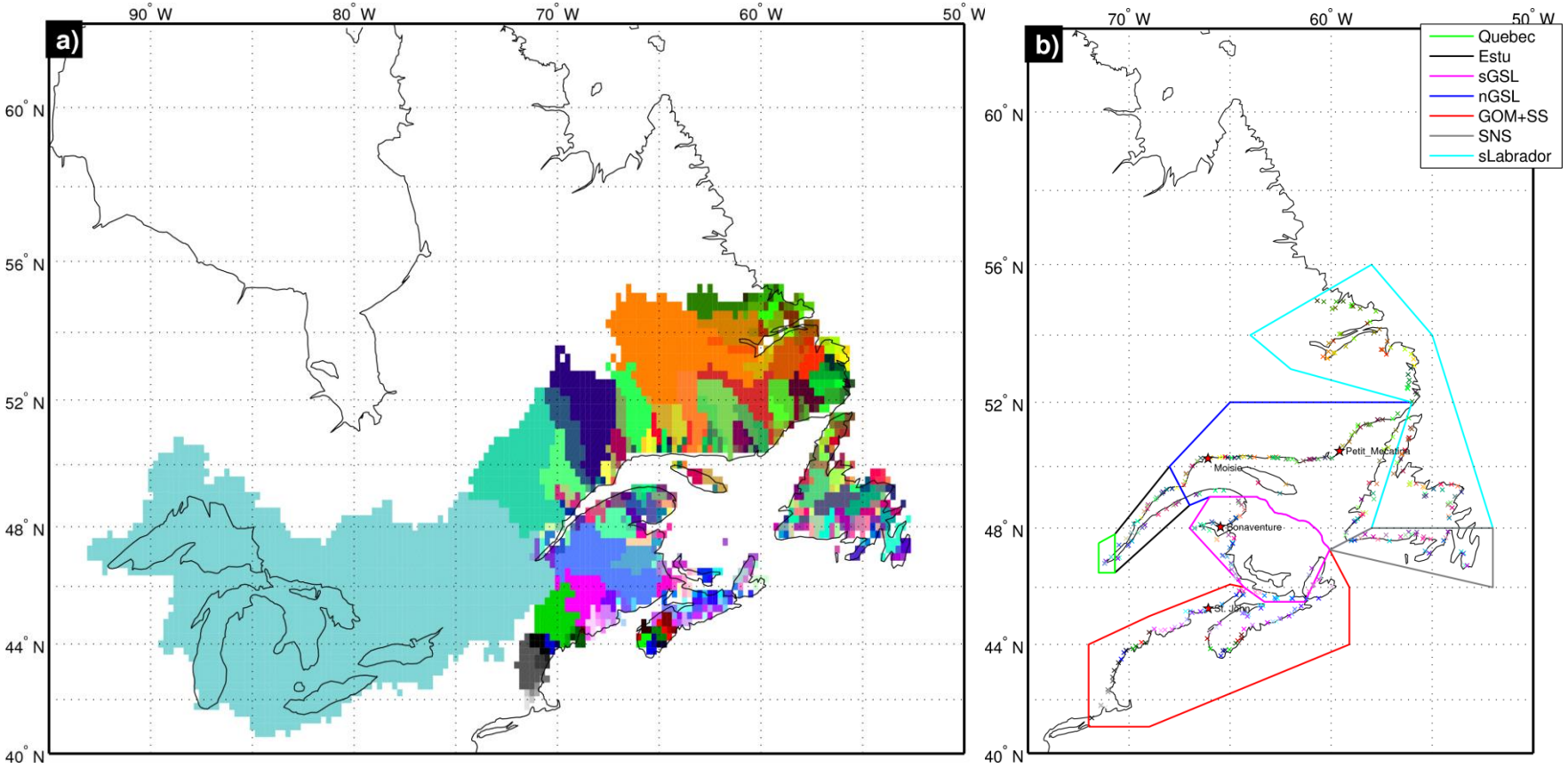

Figure 5. a) Map of the modeled watersheds of the 346 rivers in the domain.
b) Position of the river mouths (x) and the zones (colored polygons) used for the calculation of the runoff. The stars show the positions of the rivers mentioned in the Figure 4.

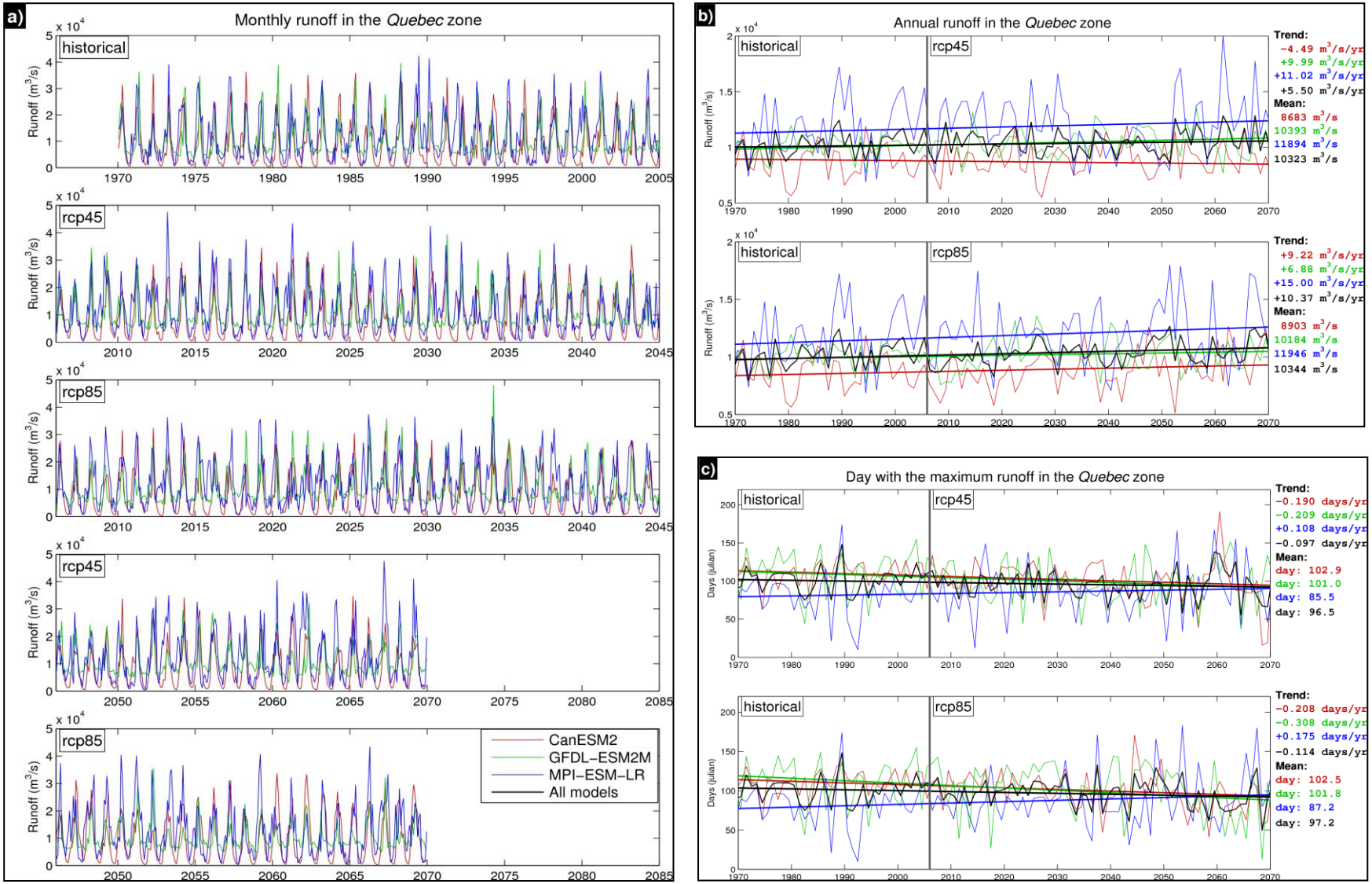

Figure 6. a) Time series of the monthly mean runoff in the *Quebec* zone calculated with the runoff flux of the three global models (CanESM2, GFDL-ESM2M and MPI-ESM-LR) with two projection scenarios (RCP 4.5 and RCP 8.5). The black line (shown in b and c) represents the average of the three global models.
b) Time series of the yearly mean runoff in the *Quebec* zone with the global trend for 1970-2070.
c) Time series of the Julian day with the maximum runoff of the year in the *Quebec* zone. The series was filtered with a moving average of seven days.

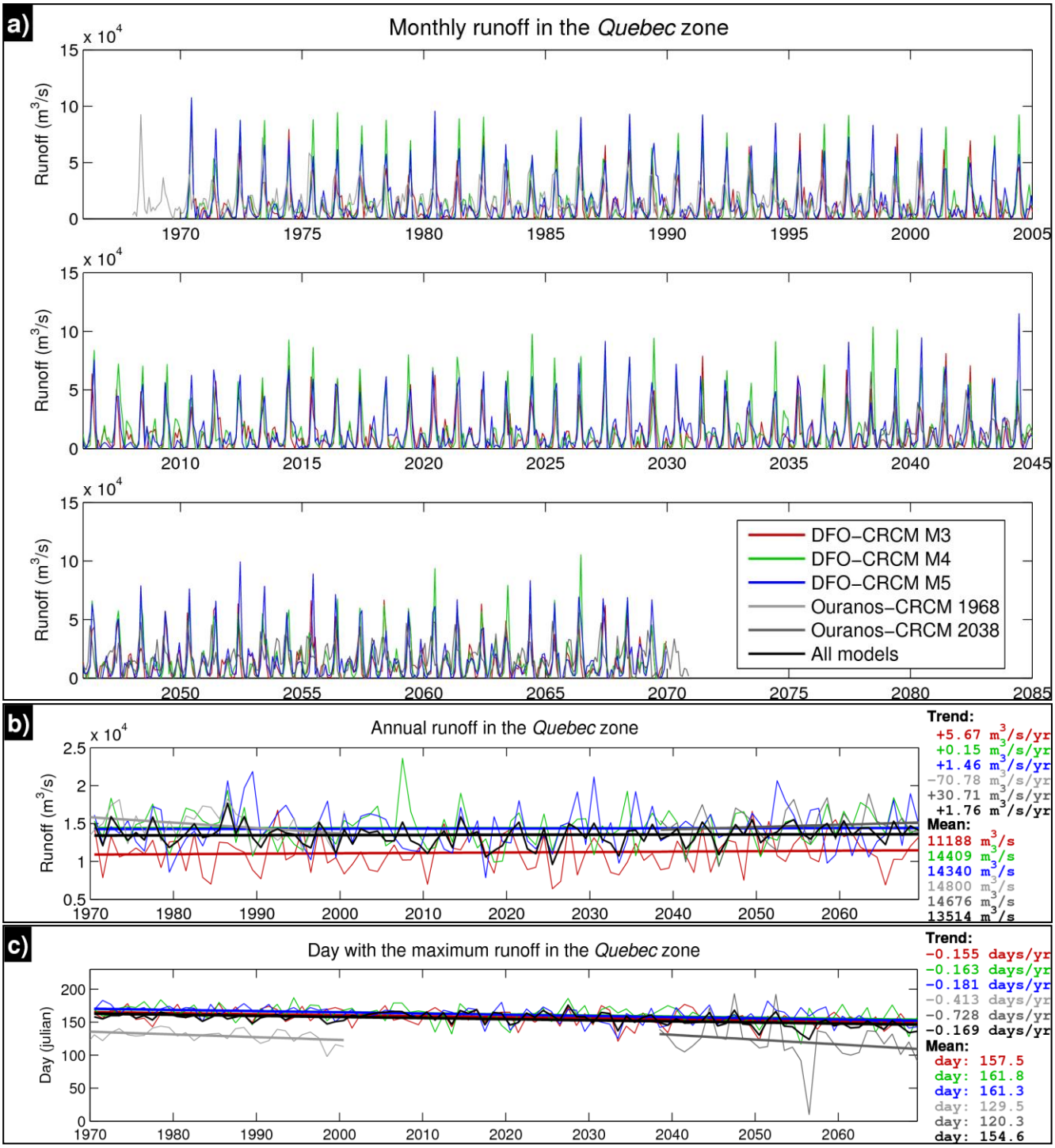

Figure 7. a) Time series of the monthly mean runoff in the *Quebec* zone calculated considering precipitation, evaporation and temperature from the regional models: DFO-CRCM (scenario A1B, members M3, M4 and M5) and Ouranos-CRCM (scenario A2, periods 1968-2000 and 2038-2070). The black line (shown in b and c) represents the average of the two regionals models or only the DFO-CRCM when there was no data from Ouranos-CRCM.
b) Time series of the yearly mean runoff in the *Quebec* zone with the global trend for 1970-2070 using the DFO-CRCM and for the two periods of 33 years using the Ouranos-CRCM model.
c) Time series of the Julian day of the maximum runoff of the year in the *Quebec* zone. The series was filtered with a moving average of seven days.

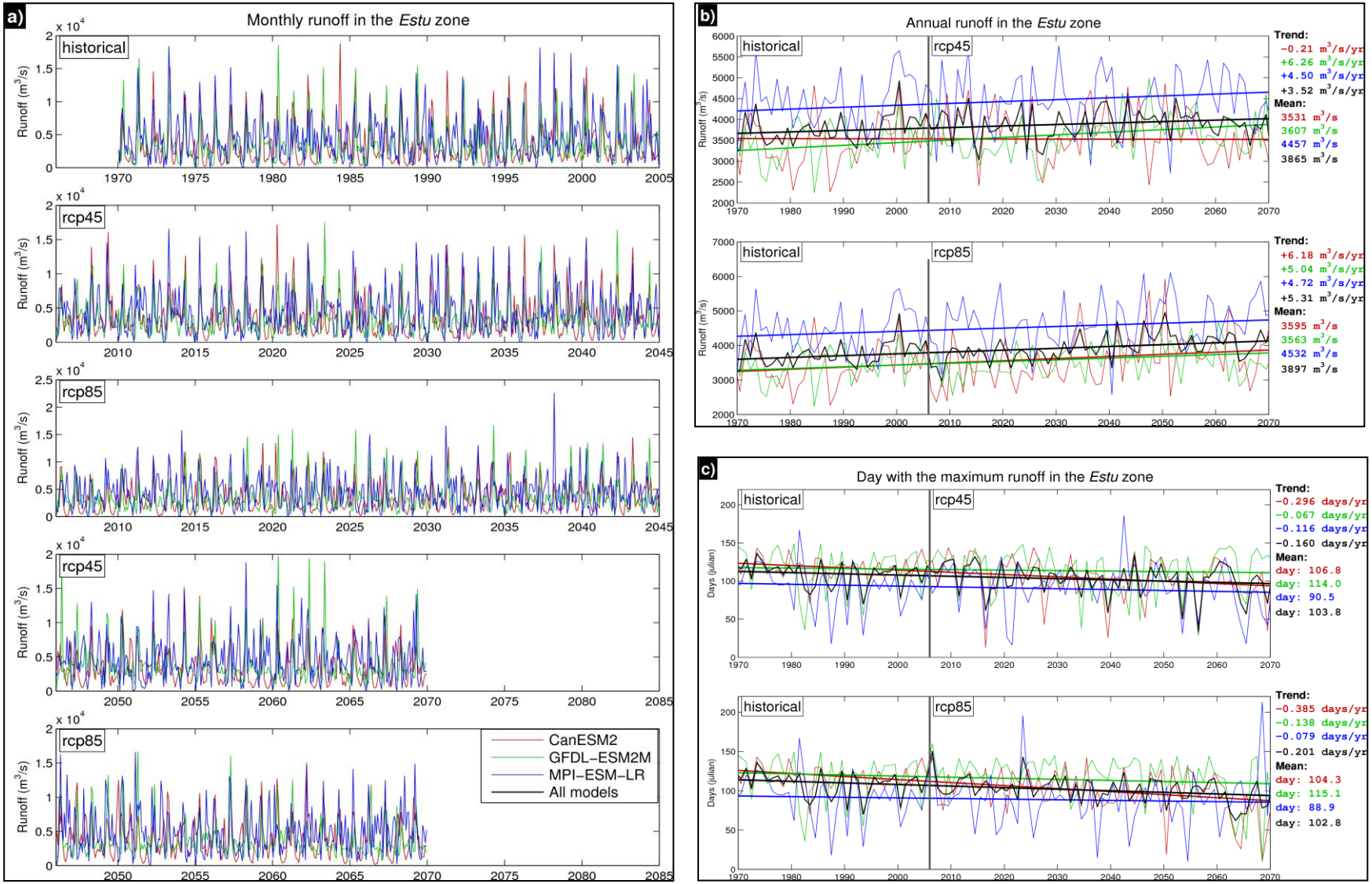

Figure 8. a) Time series of the monthly mean runoff in the *Estu* zone calculated with the runoff flux of the three global models (CanESM2, GFDL-ESM2M and MPI-ESM-LR) with two projection scenarios (RCP 4.5 and RCP 8.5). The black line (shown in b and c) represents the average of the three global models.

b) Time series of the yearly mean runoff in the *Estu* zone with the global trend for 1970-2070.

c) Time series of the Julian day with the maximum runoff of the year in the *Estu* zone. The series was filtered with a moving average of seven days.

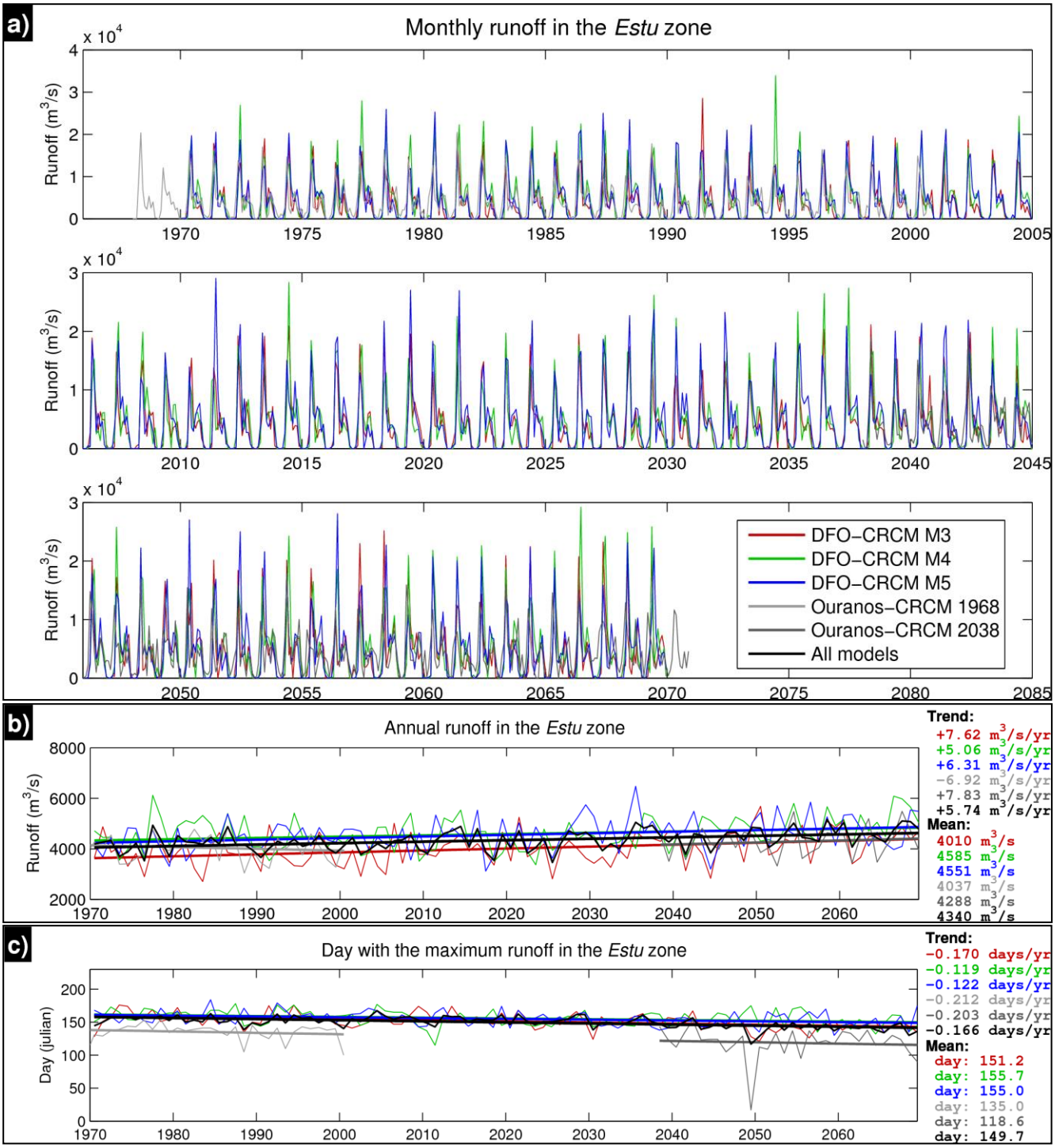

Figure 9. a) Time series of the monthly mean runoff in the *Estu* zone calculated considering precipitation, evaporation and temperature from the regional models: DFO-CRCM (scenario A1B, members M3, M4 and M5) and Ouranos-CRCM (scenario A2, periods 1968-2000 and 2038-2070). The black line (shown in b and c) represents the average of the two regionals models or only the DFO-CRCM when there is no data from Ouranos-CRCM.
b) Time series of the yearly mean runoff in the *Estu* zone with the global trend for 1970-2070 using the CRCM and for the two periods of 33 years using the Ouranos-CRCM model.
c) Time series of the Julian day with the maximum runoff of the year in the *Estu* zone. The series was filtered with a moving average of seven days.

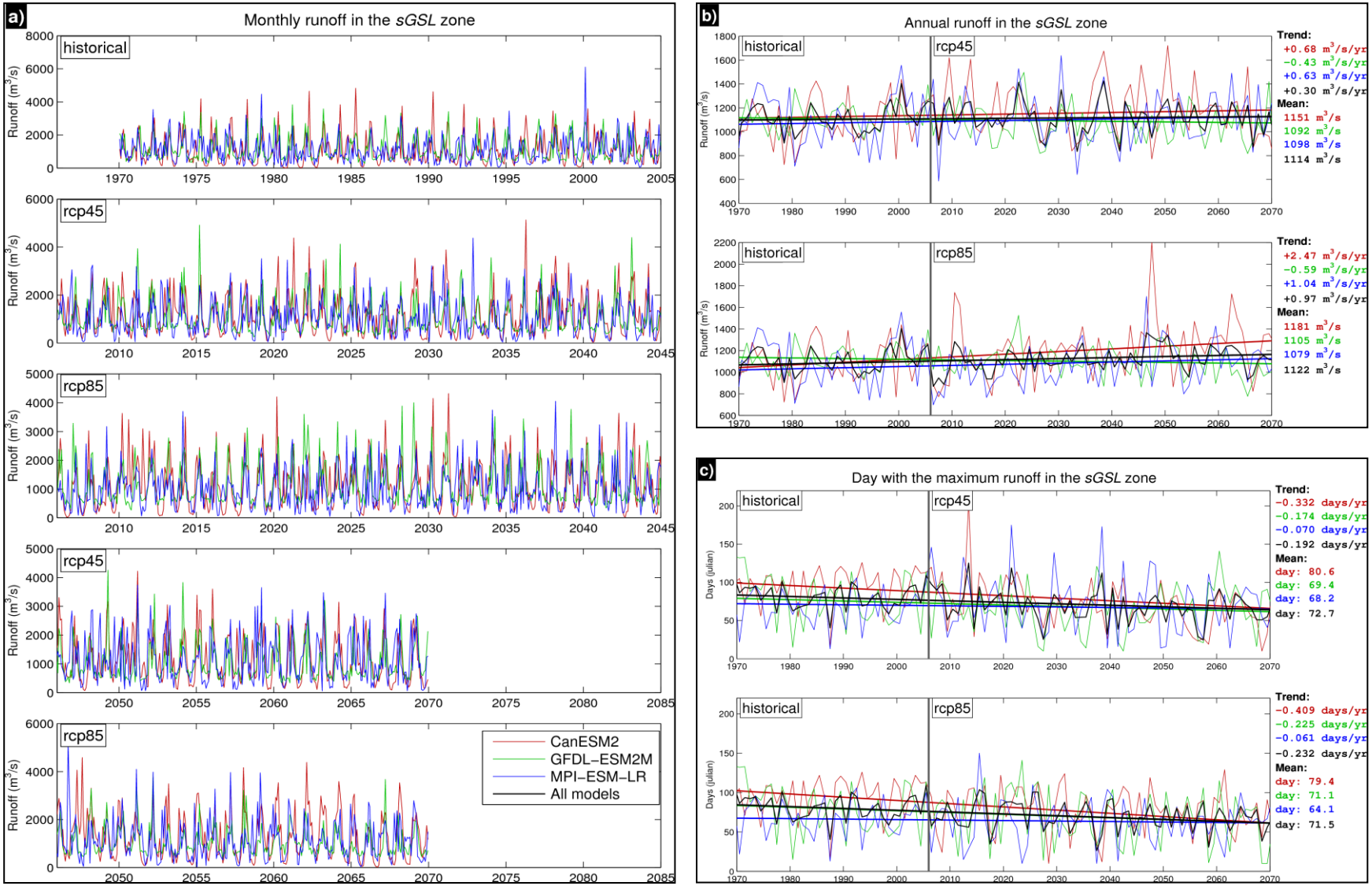

Figure 10.a) Time series of the monthly mean runoff in the *sGSL* zone calculated with the runoff flux of the three global models (CanESM2, GFDL-ESM2M and MPI-ESM-LR) with two projection scenarios (RCP 4.5 and RCP 8.5). The black line (shown in b and c) represents the average of the three global models.

b) Time series of the yearly mean runoff in the *sGSL* zone with the global trend for 1970-2070.

c) Time series of the Julian day with the maximum runoff of the year in the *sGSL* zone. The series was filtered with a moving average of seven days.

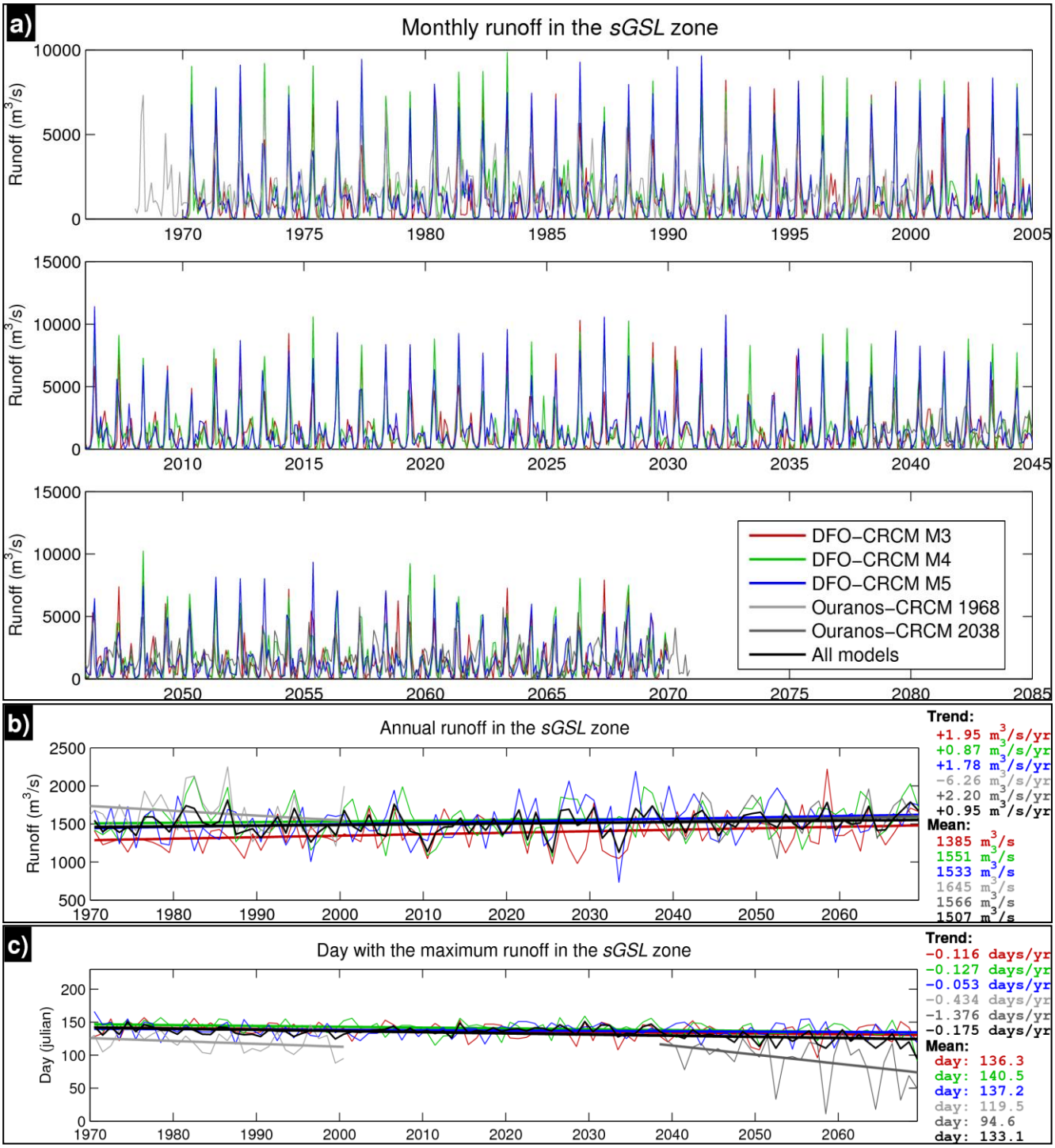

Figure 11. a) Time series of the monthly mean runoff in the *sGSL* zone calculated considering precipitation, evaporation and temperature from the regional models: DFO-CRCM (scenario A1B, members M3, M4 and M5) and Ouranos-CRCM (scenario A2, periods 1968-2000 and 2038-2070). The black line (shown in b and c) represents the average of the two regionals models or only the DFO-CRCM when there was no data from Ouranos-CRCM.
b) Time series of the yearly mean runoff in the *sGSL* zone with the global trend for 1970-2070 using the CRCM and for the two periods of 33 years using the Ouranos-CRCM.
c) Time series of the Julian day of the maximum runoff of the year in the *sGSL* zone. The series was filtered with a moving average of seven days.

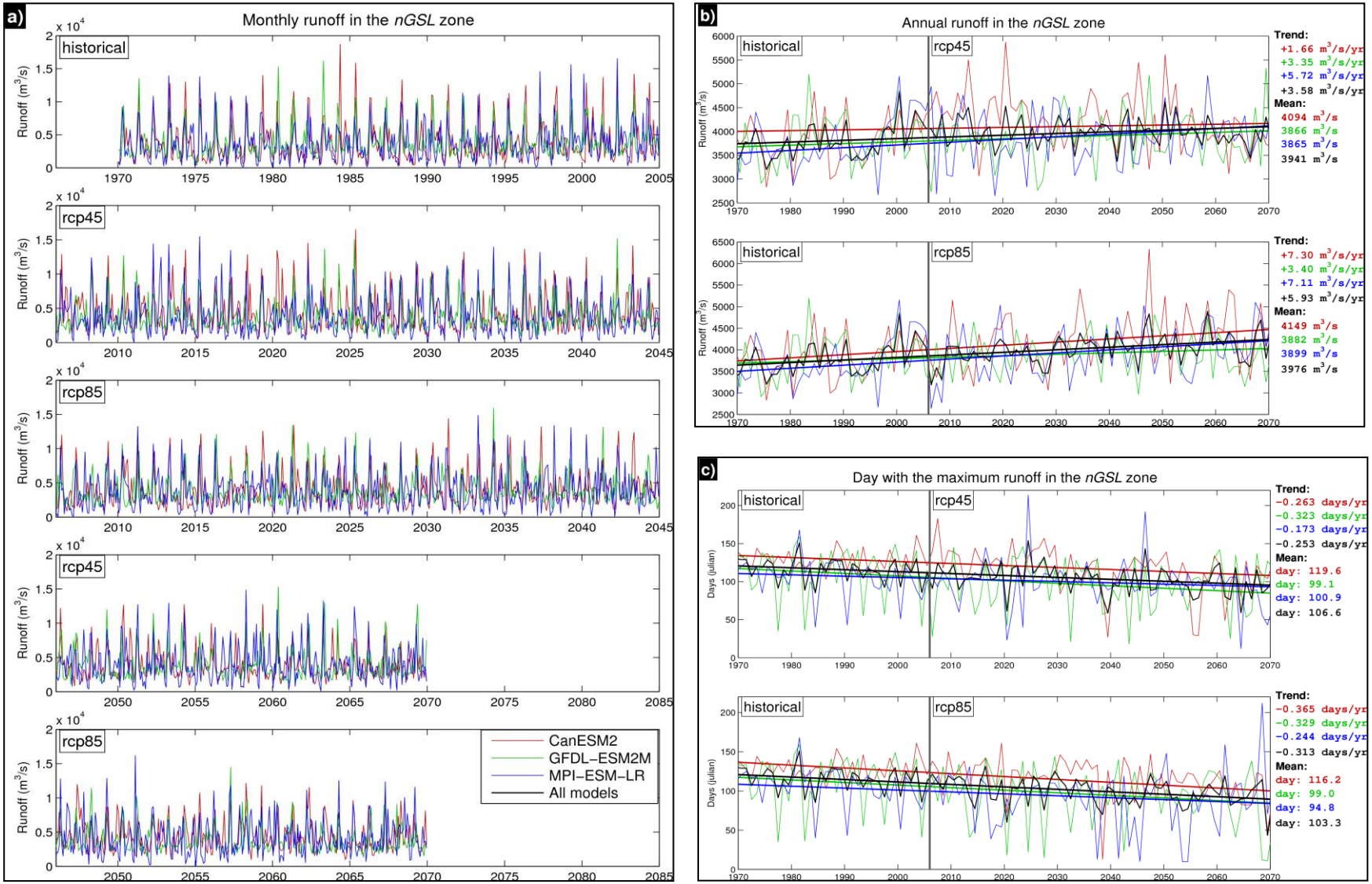

Figure 12. a) Time series of the monthly mean runoff in the *nGSL* zone calculated with the runoff flux of the three global models (CanESM2, GFDL-ESM2M and MPI-ESM-LR) with two projection scenarios (RCP 4.5 and RCP 8.5). The black line (shown in b and c) represents the average of the three global models.
b) Time series of the yearly mean runoff in the *nGSL* zone with the global trend for 1970-2070.
c) Time series of the Julian day with the maximum runoff of the year in the *nGSL* zone. The series was filtered with a moving average of seven days.

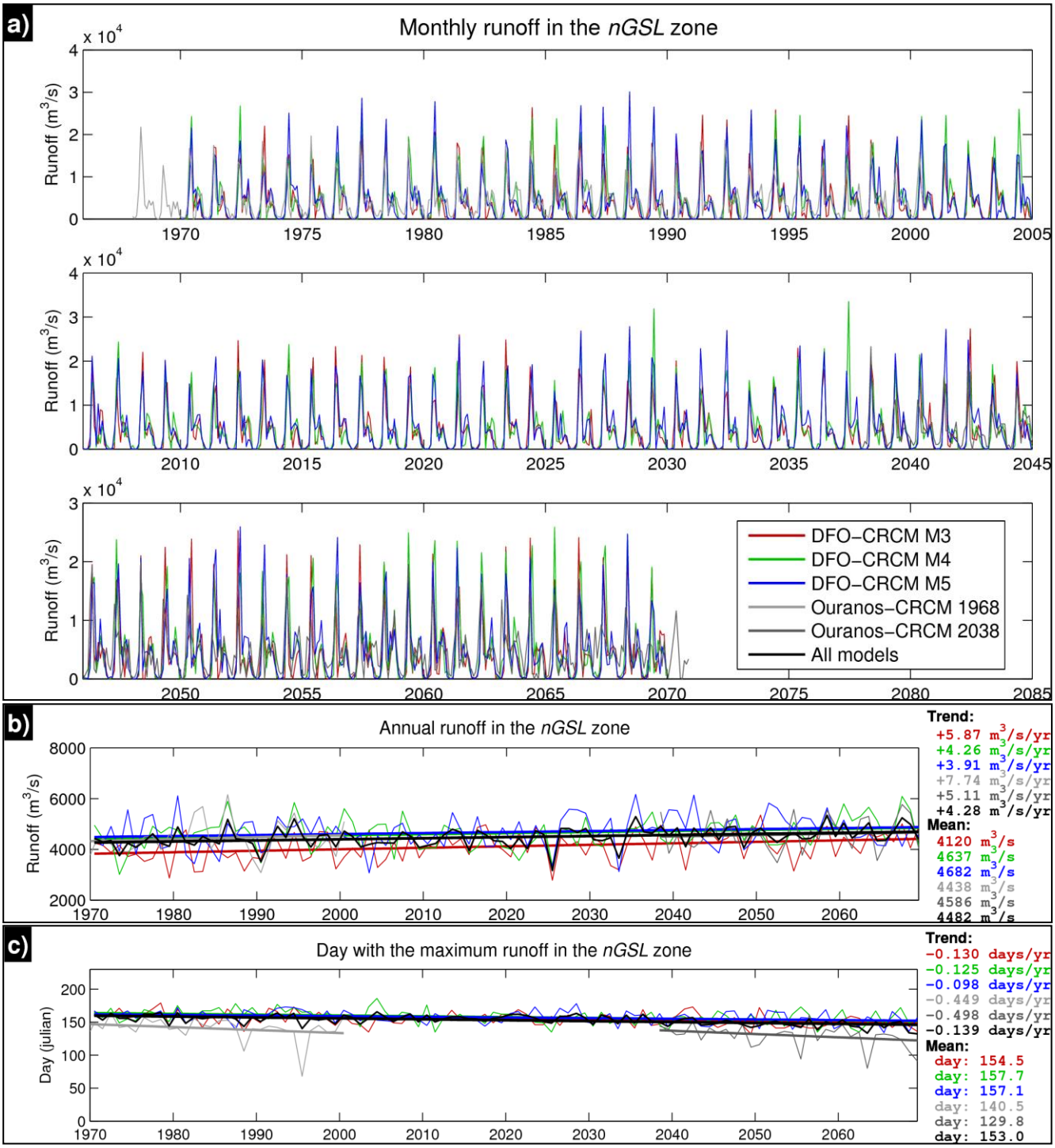

Figure 13. a) Time series of the monthly mean runoff in the *nGSL* zone calculated considering precipitation, evaporation and temperature from the regional models: DFO-CRCM (scenario A1B, members M3, M4 and M5) and Ouramos-CRCM (scenario A2, period 1968-2000 and 2038-2070). The black line (shown in b and c) represents the average of the two regionals models or only the DFO-CRCM when there was no data from Ouranos-CRCM.
b) Time series of the yearly mean runoff in the *nGSL* zone with the global trend for 1970-2070 using the CRCM and for the two periods of 33 years using the Ouranos-CRCM.
c) Time series of the Julian day of the maximum runoff of the year in the *nGSL* zone. The series was filtered with a moving average of seven days.

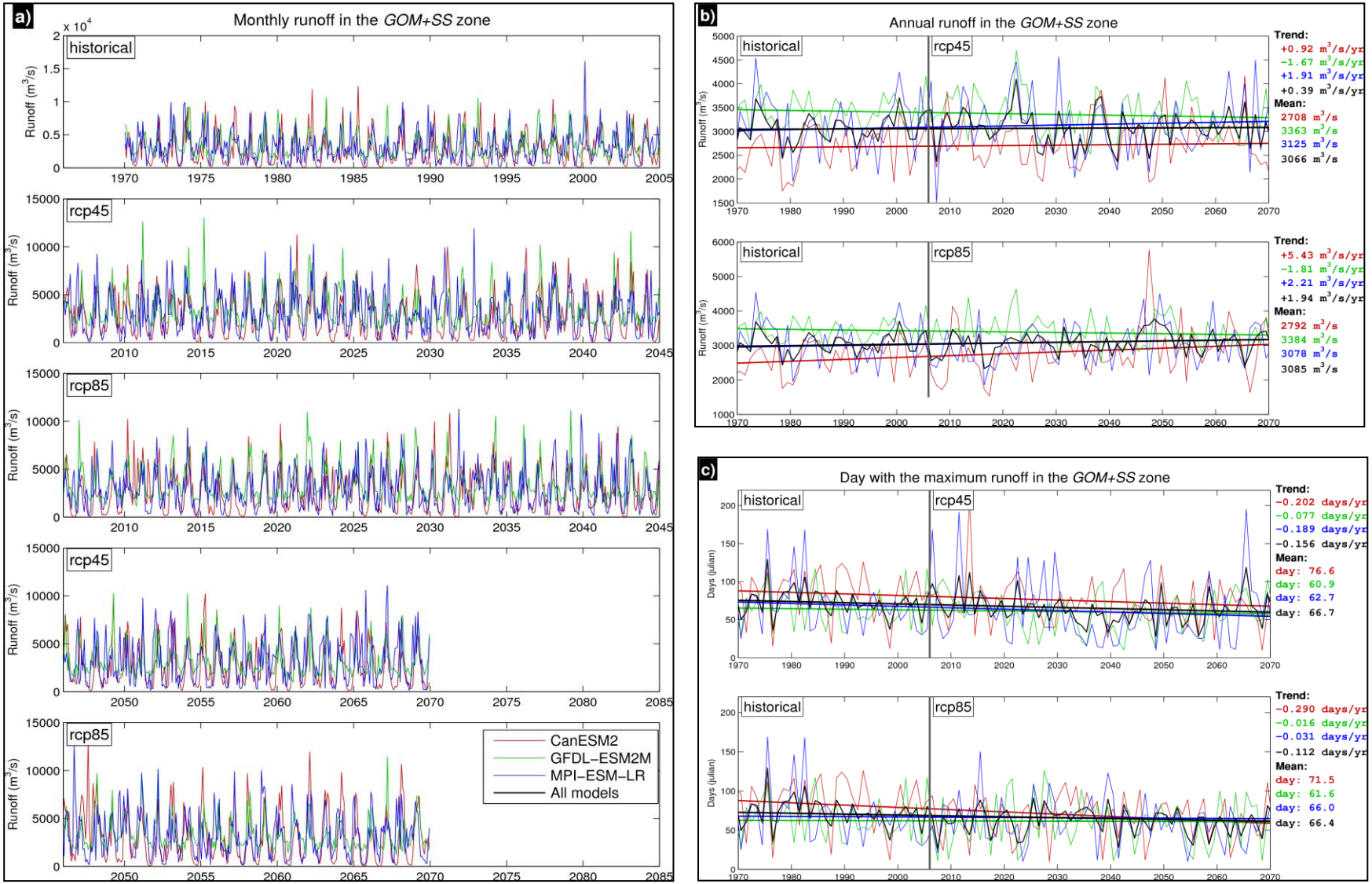

Figure 14. a) Time series of the monthly mean runoff in the *GOM+SS* zone calculated with the runoff flux of the three global models (CanESM2, GFDL-ESM2M and MPI-ESM-LR) with two projection scenarios (RCP 4.5 and RCP 8.5). The black line (shown in b and c) represents the average of the three global models.
b) Time series of the yearly mean runoff in the *GOM+SS* zone with the global trend for 1970-2070.
c) Time series of the Julian day with the maximum runoff of the year in the *GOM+SS* zone. The series was filtered with a moving average of seven days.

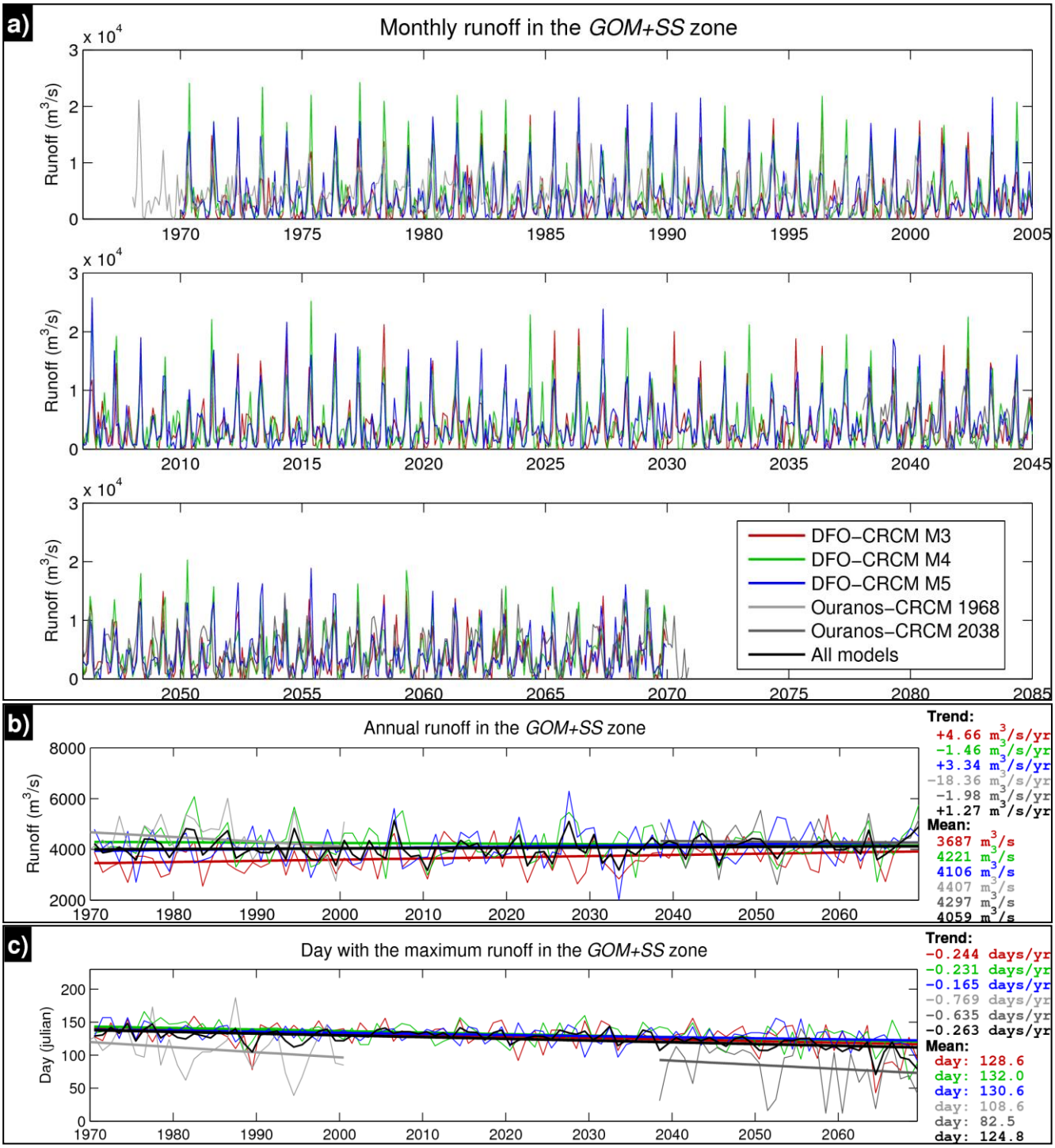

Figure 15. a) Time series of the monthly mean runoff in the *GOM+SS* zone calculated considering precipitation, evaporation and temperature from the regional models: DFO-CRCM (scenario A1B, member M3, M4 and M5) and Ouranos-CRCM (scenario A2, periods 1968-2000 and 2038-2070). The black line (shown in b and c) represents the average of the two regionals models or only the DFO-CRCM when there was no data from Ouranos-CRCM.
b) Time series of the yearly mean runoff in the *GOM+SS* zone with the global trend for 1970-2070 using the DFO-CRCM and for the two periods of 33 years using the Ouranos-CRCM.
c) Time series of the Julian day of the maximum runoff of the year in the *GOM+SS* zone. The series was filtered with a moving average of seven days.

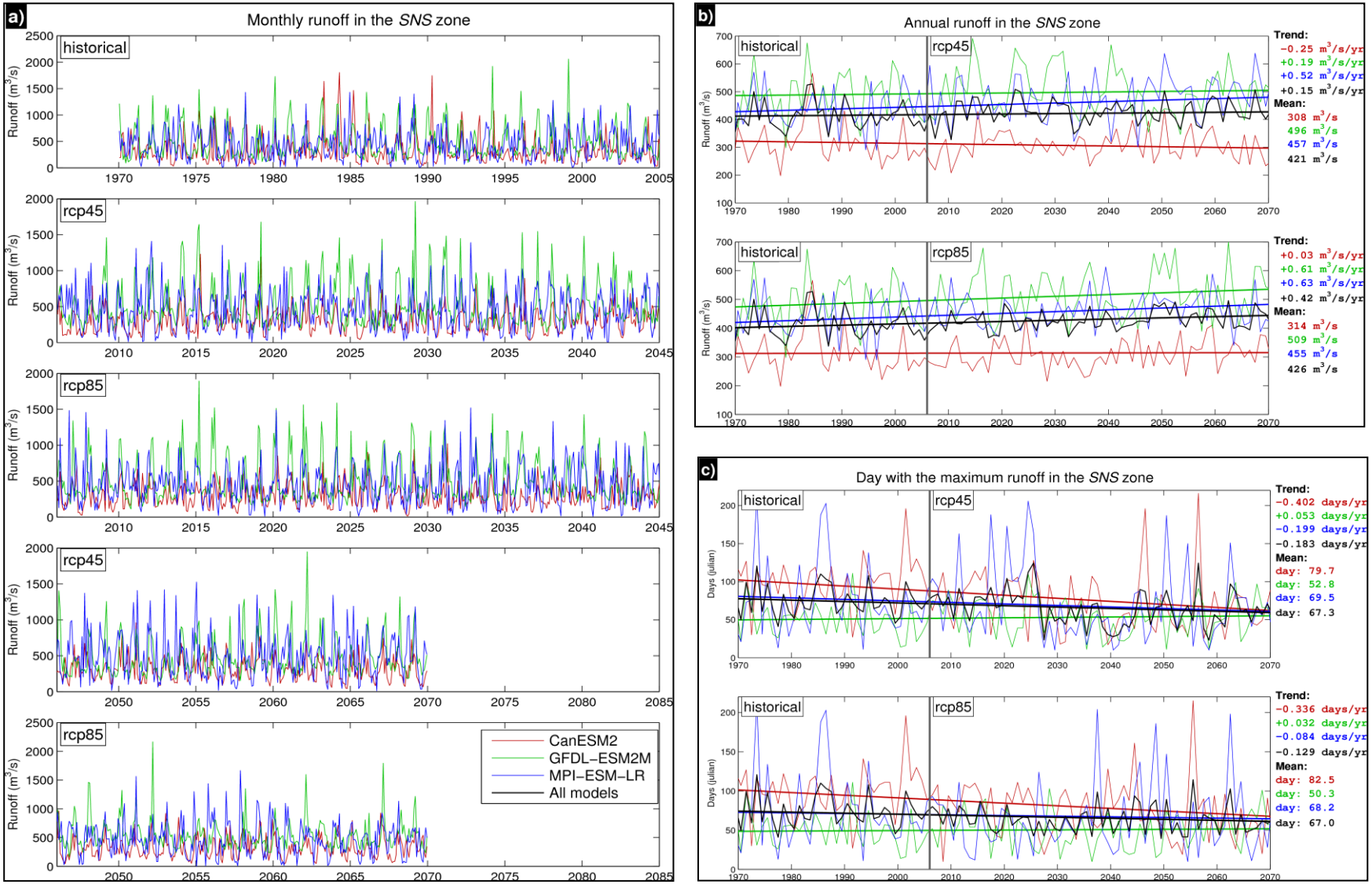

Figure 16. a) Time series of the monthly mean runoff in the *SNS* zone calculated with the runoff flux of the three global models (CanESM2, GFDL-ESM2M and MPI-ESM-LR) with two projection scenarios (RCP 4.5 and RCP 8.5). The black line (shown in b and c) represent the averages of the three global models.

b) Time series of the yearly mean runoff in the *SNS* zone with the global trend for 1970-2070.

c) Time series of the Julian day with the maximum runoff of the year in the *SNS* zone. The series was filtered with a moving average of seven days.

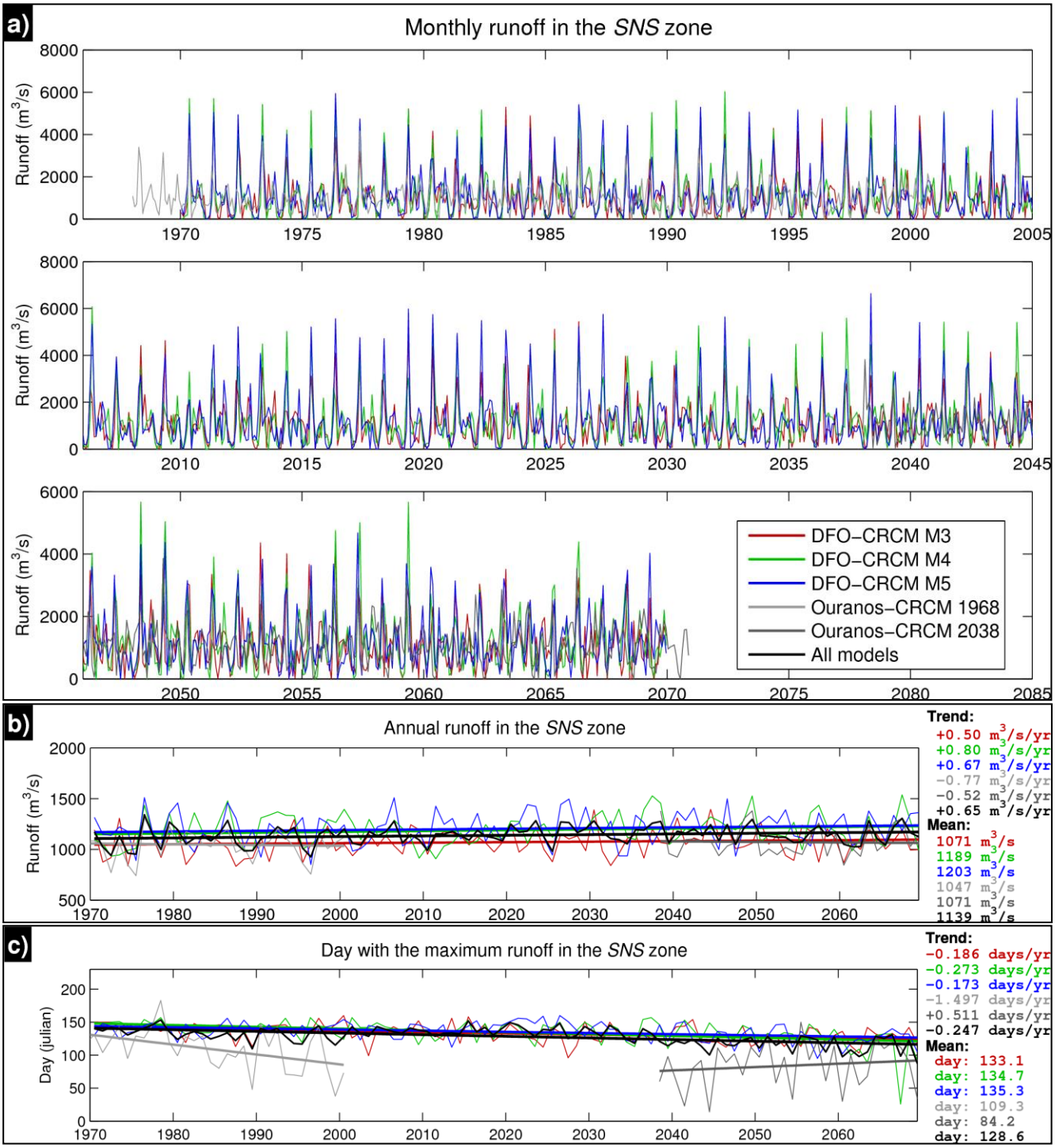

Figure 17. a) Time series of the monthly mean runoff in the *SNS* zone calculated considering precipitation, evaporation and temperature from the regional models: DFO-CRCM (scenario A1B, members M3, M4 and M5) and Ouranos-CRCM (scenario A2, periods 1968-2000 and 2038-2070). The black line (shown in b and c) represents the average of the two regionals models or only the DFO-CRCM when there was no data from Ouranos-CRCM.
b) Time series of the yearly mean runoff in the *SNS* zone with the global trend for 1970-2070 using the DFO-CRCM and for the two periods of 33 years using the Ouranos-CRCM.
c) Time series of the Julian day of the maximum runoff of the year in the *SNS* zone. The series was filtered with a moving average of seven days.

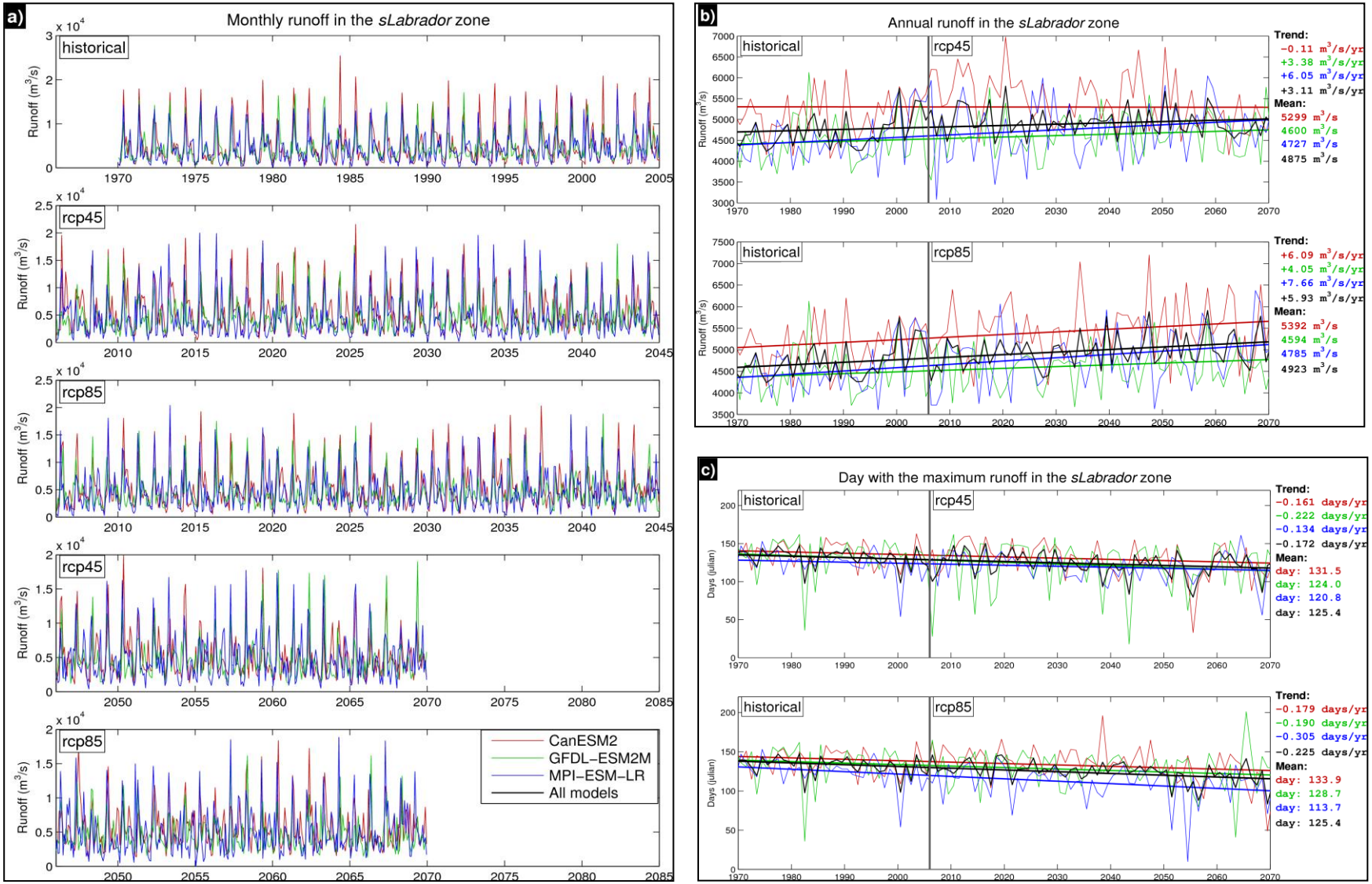

Figure 18. a) Time series of the monthly mean runoff in the *sLabrador* zone calculated with the runoff flux of the three global models (CanESM2, GFDL-ESM2M and MPI-ESM-LR) with two projection scenarios (RCP 4.5 and RCP 8.5). The black line (shown in b and c) represents the average of the three global models.

b) Time series of the yearly mean runoff in the *sLabrador* zone with the global trend for 1970-2070.

c) Time series of the Julian day with the maximum runoff of the year in the *sLabrador* zone. The series was filtered with a moving average of seven days.

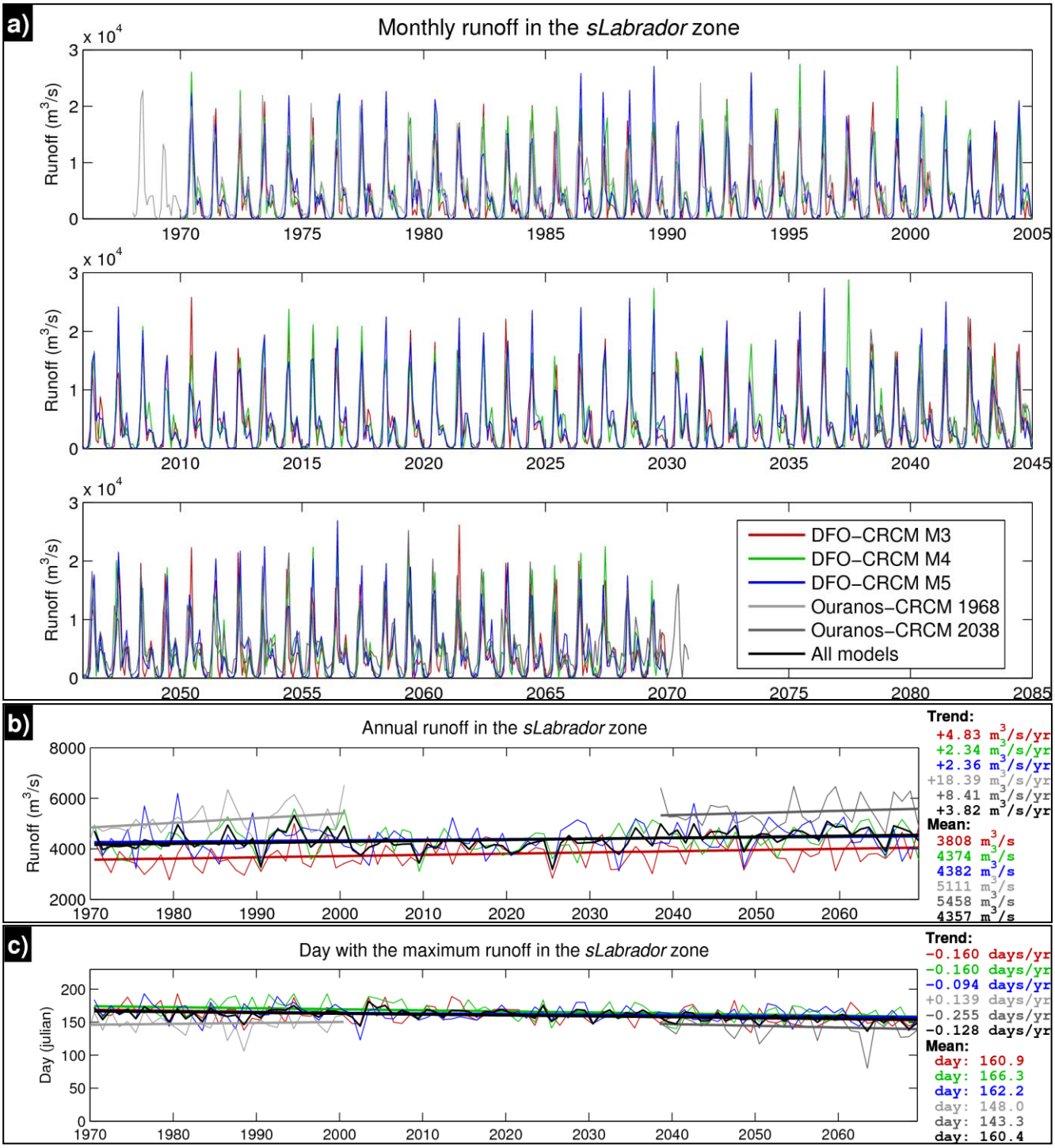

Figure 19. a) Time series of the monthly mean runoff in the *sLabrador* zone calculated considering precipitation, evaporation and temperature from the regional models: DFO-CRCM (scenario A1B, members M3, M4 and M5) and Ouranos-CRCM (scenario A2, periods 1968-2000 and 2038-2070). The black line (shown in b and c) represents the average of the two regionals models or only the DFO-CRCM when there was no data from Ouranos-CRCM.
b) Time series of the yearly mean runoff in the *sLabrador* zone with the global trend for 1970-2070 using the DFO-CRCM and for the two periods of 33 years using the Ouranos-CRCM.
c) Time series of the Julian day of the maximum runoff of the year in the *sLabrador* zone. The series was filtered with a moving average of seven days.

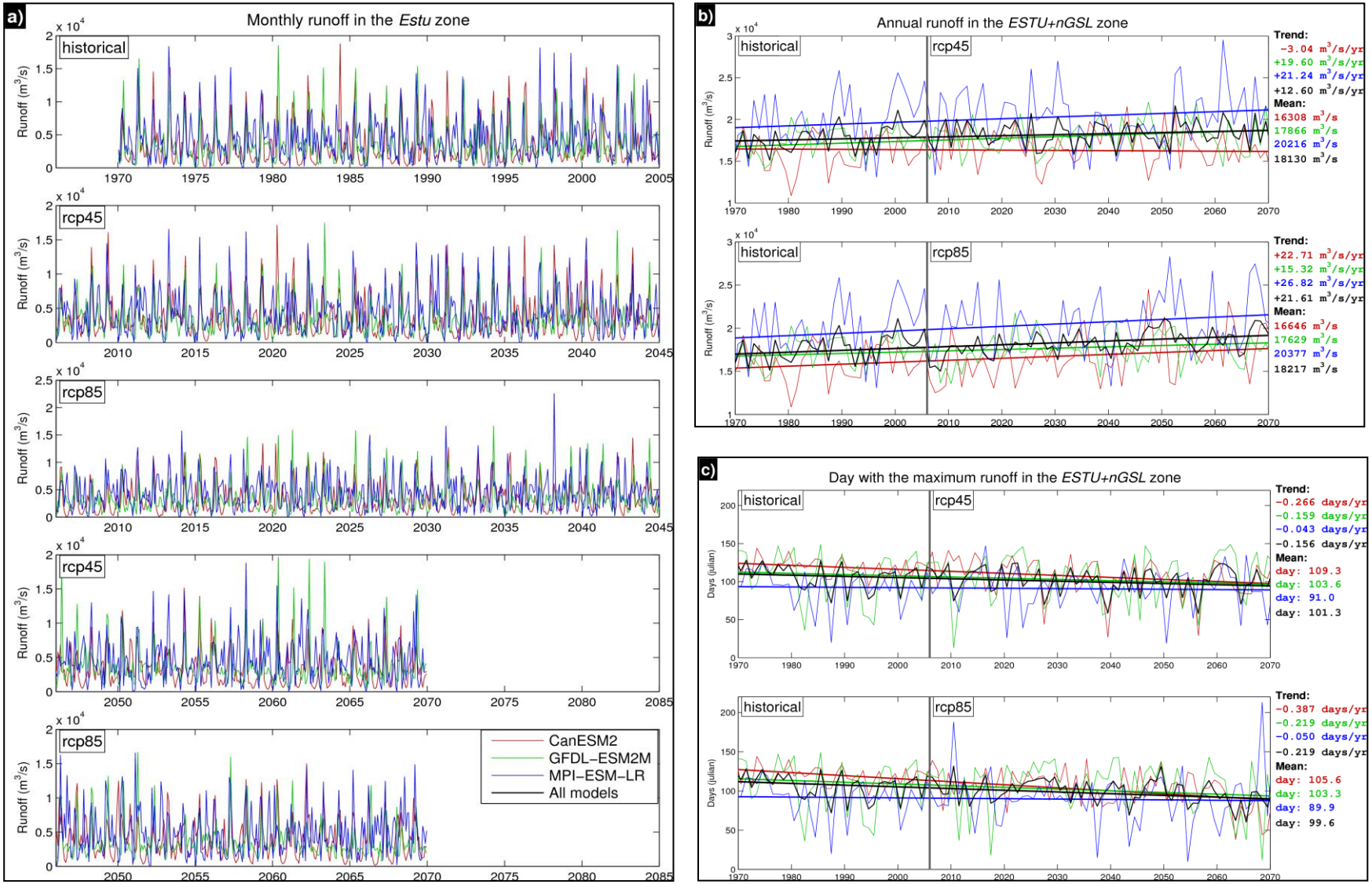

Figure 20. a) Time series of the monthly mean runoff in the ESTU+nGSL zone calculated with the runoff flux of the three global models (CanESM2, GFDL-ESM2M and MPI-ESM-LR) with two projection scenarios (RCP 4.5 and RCP 8.5). The black line (shown in b and c) represents the average of the three global models.

b) Time series of the yearly mean runoff in the ESTU+nGSL zone with the global trend for 1970-2070.

c) Time series of the Julian day with the maximum runoff of the year in the ESTU+nGSL zone. The series was filtered with a moving average of seven days.

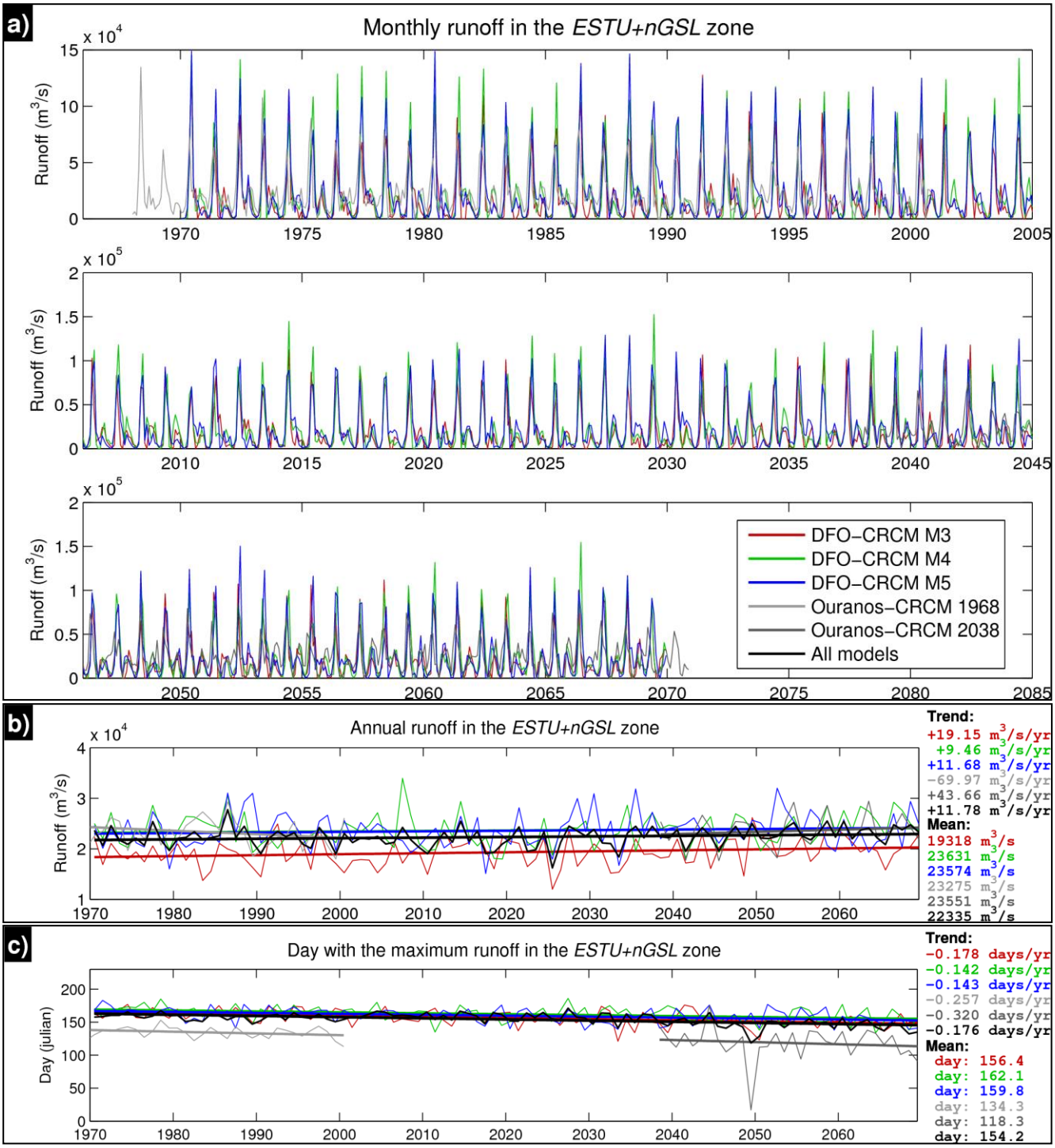

Figure 21. a) Time series of the monthly mean runoff in the *ESTU+nGSL* zone calculated considering precipitation, evaporation and temperature from the regional models: CRCM (scenario A1B, members M3, M4 and M5) and CRCM2 (scenario A2, periods 1968-2000 and 2038-2070). The black line (shown in b and c) represents the average of the two regionals models or only the DFO-CRCM when there was no data from Ouranos-CRCM.
b) Time series of the yearly mean runoff in the *ESTU+nGSL* zone with the global trend for 1970-2070 using the CRCM model and for the two periods of 33 years using the CRCM2 model.
c) Time series of the Julian day of the maximum runoff of the year in the *ESTU+nGSL* zone. The series was filtered with a moving average of seven days.